

Carbon isotopes, ammonites and earthquakes: Key Triassic–Jurassic boundary events in the coastal sections of south-east County Antrim, Northern Ireland, UK

Andrew J. Jeram^{a,*}, Michael, J. Simms^b, Stephen P. Hesselbo^c and Robert Raine^d

^a 17 Balfour Avenue, Whitehead, County Antrim, BT38 9RD, U.K.

e-mail: andyjmail@btinternet.com

^b National Museums Northern Ireland, Cultra, Holywood, BT18 0EU, U.K.

e-mail: michael.simms@nmni.com

^c Camborne School of Mines and Environment and Sustainability Institute, University of Exeter, Penryn Campus, Penryn, Cornwall TR10 9FE, U.K.

^d Geological Survey of Northern Ireland, Dundonald House, Belfast BT4 3SB, U.K.

Key Words: Rhaetian, Hettangian, mass extinction, large igneous province, carbon isotopes, seismites, correlation, Triassic–Jurassic boundary, $p\text{CO}_2$

ABSTRACT

1 A continuous succession of marine and marginal-marine sediments of Rhaetian (Late Triassic) and
2 Hettangian (Early Jurassic) age is present in the Larne Basin in Northern Ireland. These strata cover a period
3 in Earth's history that included the emplacement of the Central Atlantic Magmatic Province (CAMP), the
4 End Triassic mass Extinction (ETE), the Triassic–Jurassic boundary (TJB) and major perturbations in the
5 global carbon cycle. The Waterloo Bay section in the Larne Basin offers a well exposed record of sediments
6 that span this interval, and it has previously been proposed as a candidate GSSP for the base of the Jurassic.
7 A high-resolution $\delta^{13}\text{C}_{\text{org}}$ and organic carbon record for this locality is presented here, with these new data
8 tied to previous stratigraphic descriptions, ammonite biostratigraphy, atmospheric carbon dioxide
9 concentration ($p\text{CO}_2$) reconstructions, and nearby borehole sections that do not suffer from the thermal
10 alteration that has affected the Waterloo Bay section. Several new exposures, unaffected by thermal
11 metamorphism, are described that could provide future palynological and micropalaentological studies
12 across this important boundary interval. Correlation is established between the well-studied sections in North

13 Somerset and the likely position of the TJB in the Larne Basin is discussed. Records of soft sediment
14 deformation, synsedimentary fault movement, relative sea-level change and their likely causes are discussed.
15

1. Introduction

16 The Triassic–Jurassic transition coincides with the onset of Pangaeian break-up and development of the
17 Central Atlantic Magmatic Province (CAMP) in the main rift zone (Rhul et al., 2020 and references therein).
18 The volcanism generated $\sim 2\text{--}4 \times 10^6 \text{ km}^3$ of flood basalts (McHone, 2003) and huge volumes of CO_2 , SO_2
19 and other gases (Svensen et al., 2007; Korte et al., 2009, 2019; Bond and Wignall, 2014; Heimdal et al.,
20 2018, 2019) over a period of $\sim 500\text{--}600 \text{ ka}$, with a particularly intense early pulse concentrated in just 60 ka
21 (Blackburn et al., 2013; Korte et al., 2019).

22 The CAMP volcanism had a global impact on ocean–atmosphere chemistry and probably influenced both the
23 climate and biosphere, and also the End Triassic mass extinction (ETE) (Whiteside et al., 2010; Pálffy and
24 Kocsis, 2014). There is evidence for major biotic turnover in the latest Triassic (Bond and Wignall, 2014;
25 McElwain et al., 1999, 2009; Wignall and Atkinson, 2020), but questions remain about the timing, duration
26 and causes of diversity loss (Lucas and Tanner, 2015; Onoue et al., 2016) and there is still room for
27 scepticism (e.g. Smith and McGowan, 2007; Lucas and Tanner, 2008, 2015; Fox et al., 2020).

28 Linking abiotic events to biotic change requires a precise temporal framework based upon accurate, reliable
29 and precise stratigraphic correlation. Biostratigraphy, traditionally considered a primary correlation tool in
30 the Phanerozoic, can prove challenging when the biota is of low-diversity, sparse and in flux (as in the wake
31 of a mass extinction). Across the Triassic–Jurassic Boundary (TJB) interval, in particular where there is an
32 absence (as in the UK) of key boundary marker ammonoids such as *Psiloceras spelae* Guex, carbon isotope
33 stratigraphy has increasingly come to the fore as a correlation tool (Korte et al., 2019; Ruhl et al., 2020).

34 One of the first high-resolution carbon isotope records to be documented through the TJB interval was from
35 St Audrie’s Bay, North Somerset in south-west Britain (Hesselbo et al., 2002). Considered to preserve the
36 most complete marine succession through this interval in the U.K., this section was proposed as a candidate
37 for the base-Hettangian GSSP (Warrington et al., 1994, 2008). Even now it remains a widely used reference
38 section because the position of the ‘initial’ and ‘main’ negative Carbon Isotope Excursions (CIEs) have been
39 established relative to magnetostratigraphic, cyclostratigraphic and biostratigraphic records from the same
40 section and hence can be correlated more readily with many TJB marine successions than can the TJB GSSP
41 (Global Stratotype Section and Point) at Kujoch, Austria (Hillebrandt et al., 2013). However, this view is not
42 universally held and Fox et al. (2020) have recently cast doubt on the nature of the C-isotope signal at St
43 Audrie’s Bay, North Somerset (and by inference other UK curves), attributing it to the biotic effects of sea-
44 level change, rather than reflecting exogenous sources of carbon.

45 Regardless of the cause of isotope excursions, correlation of carbon isotope curves also has its issues.
46 Sedimentation rates and the relative contributions of terrestrial and marine organic matter may vary both
47 within and between sections (Schobben et al., 2019). Even at St Audrie's Bay several different positions
48 have been proposed for the TJB, based upon various interpretations of the isotope profiles from the Austrian
49 GSSP and sections in the Americas (Guex et al., 2004; Thibodeau et al., 2016, Yager et al., 2017; Wignall
50 and Atkinson, 2020). Without clear consensus, global correlation of the TJB remains in doubt, as does the
51 reliability of the CAMP/ETE stratigraphic framework which has depended heavily upon the St Audrie's Bay
52 stratigraphic record. A near identical carbon isotope curve to that at St Audrie's Bay has been recorded from
53 Doniford Bay (Clémence et al., 2010), just 2 km to the west, but few other carbon isotope data from this
54 interval have been published from the UK except for the Mochras borehole in North Wales (Storm et al.,
55 2020) and the Carnduff-2 borehole within the study area of this paper (Boomer et al., 2020).

56 In eastern Co. Antrim the uppermost Triassic (Lilstock Formation) and succeeding early Hettangian
57 (Waterloo Mudstone Formation) succession is substantially thicker than in North Somerset (Simms and
58 Jeram, 2007). This paper examines events recorded through this interval at several exposures on the East
59 Antrim coast, with particular emphasis on relative sea level change, depositional environments, tectonic
60 activity and ammonite biostratigraphy. Carbon-isotope data compiled for the Waterloo Bay section can be
61 compared with other curves from the nearby Carnduff-2 Borehole (Boomer et al. 2020a) as well as sections
62 in North Somerset and further afield. The stratigraphy at Waterloo Bay has been described in detail
63 previously (Simms and Jeram, 2007) but several other coastal exposures (The Gobbins, Cloughan Point,
64 Cloughfin Port) are described here for the first time.

2. Geological Context of the Larne Basin and Previous Research

65 The Larne Basin is a NE–SW trending half-graben formed by tensional reactivation of pre-existing
66 Caledonian structures during the Permian (Anderson et al., 1995; Raine et al., 2020), bounded by the
67 Southern Uplands Fault Zone to the south and the Highland Boundary Fault Zone to the north. The localities
68 described here all lie towards the southern side of the basin and together provide a transect across from the
69 centre towards the margin (Fig. 1). Cloughan Point and Cloughfin Port are located above the geophysical trace
70 of the Southern Uplands Fault Zone, along which associated faults may have been active during deposition
71 of the Penarth Group. Waterloo Bay lay closer to a depocentre and The Gobbins occupied an intermediate
72 position.

73 Basalts of the Antrim Lava Group (Paleocene) conceal much of the basin (Fig. 1), but coastal outcrops
74 expose a succession from the Mercia Mudstone Group (Late Triassic), through the Penarth Group (Rhaetian)
75 and into the Lias Group (Early Jurassic). The Lias Group of the Larne Basin extends no higher than the
76 Turner Zone, early Sinemurian (Ivimey-Cook, 1975, Boomer et al., 2020) and is succeeded unconformably
77 by the Late Cretaceous Hibernian Greensands Formation (Manning et al., 1970; Griffith and Wilson, 1982).
78 Although Mesozoic rocks of the Larne Basin were, in general, little-affected by Paleocene volcanism, much
79 of the Waterloo Bay section has been thermally altered, presumably due to a buried igneous intrusion.

80 The Rhaetian–Hettangian succession of southeast County Antrim was first investigated more than 150 years
81 ago (Portlock, 1843; Tate, 1867). Drilling of the Larne-1 Borehole (Manning and Wilson, 1975; Fig. 1, inset)
82 prompted Ivimey-Cook (1975) to review the Rhaetian and Hettangian of southeast Antrim, but poor core
83 recovery hindered correlation with surface exposures. Reid and Bancroft (1986) established Larne as the
84 type locality for the ammonite *Caloceras intermedium* (Portlock), figured type material of *Psiloceras*
85 *sampsoni* (Portlock) from the Lough Foyle Basin and mentioned *Psiloceras erugatum* (Phillips) at Larne and
86 Islandmagee. Simms (2003, 2007) described the Lilstock Formation (Cotham Member) seismites at Larne
87 and Cloghan Point, both in Co. Antrim and correlated them with other sites across the UK, including St.
88 Audrie’s Bay. Waterloo Bay was designated the type section for the Waterloo Mudstone Formation
89 (Mitchell, 2004) and proposed as a candidate GSSP for the base of the Hettangian Stage (Simms and Jeram
90 2007) which saw publication of the first detailed log and ammonite biostratigraphy of the boundary
91 succession (Simms and Jeram, 2007). Stomatal abundance in plant cuticle from the sections described here
92 has been used to assess atmospheric CO₂ concentrations (Steinthorsdottir et al., 2011), changes in the marine
93 benthos have also been investigated (Atkinson et al., 2019, Opazo and Page, 2021) and new borehole
94 material (Carnduff-1 and Carnduff-2) have been described and analysed (Boomer et al., 2020).

3. Lithostratigraphy of the Triassic–Jurassic Transition in SE County Antrim

95 Based on new information both from exposures and published work on the new boreholes (Boomer et al.
96 2020) the position of some lithostratigraphic boundaries indicated here differs from those identified
97 previously (Simms 2003, 2007; Simms and Jeram, 2007). The lithostratigraphic terminology developed in
98 south-west Britain (Warrington et al. 1980) has been applied to the Northern Ireland succession (Raine et al.
99 2020, 2021) but correlation is not always straightforward, particularly for the Lilstock Formation, due to
100 facies differences and a lack of biostratigraphic markers between south-west Britain and Northern Ireland.
101 Hence the use of common terminology in Northern Ireland and south-west Britain does not imply exact
102 chronostratigraphic equivalence.

3.1 Mercia Mudstone Group

103 The lithostratigraphy of the Mercia Mudstone Group in Northern Ireland was defined largely from boreholes
104 (Wilson and Manning, 1978, Mitchell, 2004). The Collin Glen Formation at the top of the group, considered
105 equivalent to the Blue Anchor Formation of England (Warrington et al., 1980), comprises up to 10 m of pale
106 green silty mudstone directly below the Penarth Group. At Waterloo Bay (Fig. 2) the upper ~50 m of the
107 normally red Mercia Mudstone Group comprise pale green sediments, probably due to the effects of thermal
108 alteration, making location of the lower boundary of the Collin Glen Formation difficult at this location.
109 Marine palynomorphs recovered from the Carnduff-1 borehole (Boomer et al., 2020) suggest a Rhaetian age
110 for the Collin Glen Formation.

3.2 Penarth Group

111 The Penarth Group is divided into the Westbury and Lilstock formations, (Warrington et al., 1980; Gallois,
112 2009), with its base in Northern Ireland defined by an unconformity/disconformity at the base of the
113 Westbury Formation and its top by the base of the succeeding Lias Group (Waterloo Mudstone Formation).

3.2.1 Westbury Formation

114 Shallow marine lithofacies of the Westbury Formation in Northern Ireland resemble those seen elsewhere in
115 the UK (Macquaker, 1999; Swift, 1999; Simms and Jeram, 2007), with very dark grey mudstones and shales,
116 hummocky cross-stratified sandstones, winnowed shell and vertebrate debris lags and convex-up shell
117 pavements. It represents a major palaeoenvironmental shift to marine conditions from the largely non-marine
118 facies of the Mercia Mudstone Group.

3.2.2 Lilstock Formation

119 The base of the Lilstock Formation across the UK is marked by a change from darker facies of the Westbury
120 Formation to paler mudstones and siltstones of the Cotham Member, the lower subdivision of the Lilstock
121 Formation. In south-west Britain there is usually a clear distinction between predominantly siliciclastic facies
122 in the Cotham Member and the overlying carbonate-rich Langport Member (Hallam, 1960; Swift, 1995;
123 Gallois 2009). The Cotham Member typically contains a sparse low-diversity marine fauna, with some
124 elements suggesting freshwater influence and in places it is capped by a stromatolite horizon known as the
125 Cotham Marble (Hamilton, 1961). In contrast, the fauna of the overlying Langport Member is often more
126 diverse, abundant and with stenohaline taxa such as corals and rare conodonts recorded in Britain (Swift and
127 Martill, 1999).

128 In Northern Ireland the transition from siliciclastic sediments of the Lilstock Formation (Cotham Member)
129 through to the characteristic mudstones and carbonates of the Lias Group is more gradational than the type
130 sections in south-west Britain, hence identifying a separate Langport Member in the Larne Basin is
131 considered problematic. The top of the Cotham Member is placed above the highest microbially laminated
132 limestone, where ripple cross-lamination becomes rare and the first organic-rich mudstones appear. Most of
133 the 4–6 m of mudstone-dominated sediments above the Cotham Member in the Larne Basin have a low
134 organic carbon content, reminiscent of the ‘Watchet Beds’ (Ivimey-Cook 1975) and are therefore assigned to
135 the Langport Member (Warrington et al., 1980).

3.2.2.1 Cotham Member

136 The lower part of the Cotham Member has been suggested to be a regressional shoreface equivalent of the
137 Westbury Formation (Hesselbo et al., 2004), but towards the margin of the Larne Basin this distinctive
138 lithofacies change may have been influenced as much by increasing accommodation space due to tectonic

139 movement as by eustatic sea-level change. The base of the Cotham Member in Northern Ireland is placed at
 140 the junction of a fine sandstone that overlies a light grey or thinly-stripped mudstone, although soft sediment
 141 deformation commonly blurs this boundary (Simms, 2003, 2007). The lower Cotham Member here is
 142 generally red-brown in colour and often intensely deformed, but changes abruptly to pale grey around the
 143 upper limit of intense soft sediment deformation. A thin hummocky, cross-stratified sandstone may truncate
 144 the deformed beds, with similar sandstone beds present up to 0.6 m higher within the grey mudstones.

145 The base of the upper Cotham Member here is placed at a widespread ‘mud-cracked’ emergence surface that
 146 has been correlated with a superficially similar surface in south-west Britain (Hesselbo et al., 2004). The
 147 upper Cotham Member, although containing coarser grained sediments, shows an overall fining-upward
 148 trend and is capped by thin micritic and microbially laminated limestones with calcareous mudstones. Small
 149 bivalves (*Eotrapezium* and *Protocardia*) occur sporadically throughout the Cotham Member in Northern
 150 Ireland (Ivimey-Cook, 1975; Opazo and Page, this issue), suggesting that Northern Ireland experienced
 151 greater marine influence than elsewhere in the UK (Swift and Martill, 1999), but the presence of
 152 conchostracans (*Euestheria*), aquatic liverworts (*Naiadita*) and freshwater ostracods (*Darwinula*) suggest
 153 schizohaline intervals.

3.2.2.2 Langport Member

154 The Langport Member (Warrington et al., 1980) in south-west Britain includes two dominant facies types
 155 that have, at times, been placed into their own lithostratigraphic divisions, the carbonate-dominated ‘White
 156 Lias’ and the fine-grained siliciclastic ‘Watchet Beds’ (Richardson, 1911; Gallois 2007, 2009; Hallam, 1960;
 157 Swift, 1995; Poole and Whiteman, 1966; Warrington and Ivimey-Cook, 1992). These facies are
 158 lithologically similar to the Lias Group and may, in part, be lateral equivalents (e.g. Korte et al., 2009). In
 159 Northern Ireland the Langport Member is mudstone-dominated with only subordinate siltstones and
 160 limestones, the latter probably at least partly diagenetic in origin. Limestones occur only at the base of the
 161 member in the Larne Basin but persist throughout as thin beds in the Lough Foyle Basin (Raine et al., 2021).
 162 In the Waterloo Bay section the base of the Langport Member is placed beneath Bed 8, where marine
 163 bivalves become persistent, followed by an increase in organic carbon content in Bed 9 and a coarsening-up
 164 sequence of mudstones, with thin silt laminae, capped by a bed containing gutter casts at several levels. The
 165 top of the member (Bed 14 at Waterloo Bay) is marked by an intensely-burrowed muddy siltstone, rich in
 166 bivalves.

3.3 Lias Group (Waterloo Mudstone Formation)

167 The Waterloo Mudstone Formation encompasses the entire Lias Group in Northern Ireland, although
 168 nowhere does this extend above the Pliensbachian Stage (Simms and Edmunds, 2021). In south-west Britain
 169 the base of the Lias Group is taken at an abrupt increase in total organic carbon (TOC) content relative to the
 170 Lilstock Formation (Hesselbo et al., 2004) and has been attributed to rapid flooding and establishment of

171 fully marine conditions (Hesselbo et al., 2004). A similar shift in the TOC can also be seen at Waterloo Bay
 172 and so the base of the Lias Group is taken immediately beneath Bed 15 where TOC content above is
 173 consistently close to, or greater than, 1% (Fig. 3). Across much of Britain limestone-shale alternations,
 174 significantly enhanced by diagenesis, characterise the Blue Lias Formation in the lowest part of the Lias
 175 Group (Simms et al., 2004). However, in the Larne Basin they do not appear until the latter part of the
 176 Planorbis Zone, although regular alternations of shale and calcareous mudstone suggest similar rhythmic
 177 bedding. The rarity of diagenetic limestone in the Larne Basin may reflect a higher sedimentation rate than
 178 other areas where these limestone-shale successions are well-developed, such as in south-west Britain
 179 (Weedon et al., 2018).

180

3.4 Ammonite biostratigraphy

181 Ammonites are key to correlating Jurassic successions across north-west Europe (Page, *in* Simms et al.,
 182 2004) but the controls on their presence or absence at particular levels in the succession remain unclear.
 183 Planorbis Zone ammonite faunas are better preserved in Northern Ireland than elsewhere in the UK and their
 184 stratigraphic distribution here has been documented in detail from the Waterloo Bay foreshore (Simms and
 185 Jeram, 2007) and from the nearby borehole cores from Carnduff (Boomer et al., 2020), with representative
 186 material held by National Museums Northern Ireland and figured here (Figs 4 and 5).

187 The ammonite succession recorded at Larne (Simms and Jeram, 2007) corresponds closely with that from the
 188 Carnduff-2 borehole (Boomer et al., 2020) and documented by Bloos and Page (2000), Page (*in* Simms et al.,
 189 2004) from Great Britain. Compared with other UK surface exposures, the succession here is considerably
 190 expanded and contains abundant and well-preserved ammonites at many levels rather than at the discrete
 191 narrow horizons typical elsewhere.

4. Site descriptions

4.1 Waterloo Bay, Larne

192 Waterloo Bay, located on the outskirts of Larne Town, 28 km NNE of Belfast (Fig. 1), is the finest exposure
 193 of the Lias Group (Waterloo Mudstone Formation) anywhere on the island of Ireland. It is best exposed on
 194 an intertidal platform (centred on coordinates 54° 51' 40" N, 5° 48' 22" W; Irish Grid Ref. D 409 037) where
 195 strata dip at 20–30° to the NW and provide almost continuous exposure, cut by minor faults (Fig. 2), from
 196 the upper part of the Mercia Mudstone Group, through the entire Penarth Group and into the Lias Group at
 197 least as far as the lowermost Sinemurian (Bucklandi Zone), where it is truncated by a major unconformity
 198 beneath the Hibernian Greensands Formation (Cretaceous, Cenomanian). The combined Penarth Group and
 199 Lias Group exposed here is ~115 m thick (Ivimey-Cook, 1975), compared with almost 177 m in the
 200 Carnduff-2 borehole (Boomer et al., 2020). The interval between the base of the Penarth Group and the first
 201 occurrence of the ammonite genus *Caloceras* has been described in detail in several other publications
 202 (Ivimey-Cook, 1975; Simms 2003, 2007; Simms and Jeram, 2007; Boomer et al. 2020) and so only a

203 summary of the ammonite stratigraphy is presented here. The shore and cliff lie within the Waterloo
 204 geological ASSI (Area of Special Scientific Interest), which provides legal protection for its geological
 205 heritage. Requests for permission to sample or collect from the section should be directed to the geological
 206 section of the Northern Ireland Environment Agency. National Museums Northern Ireland is the official
 207 designated repository for material collected from this site.

208 At Waterloo Bay ammonites first appear (and with some abundance) in Bed 24 (Fig. 3) and occur at many
 209 levels above this. Intensive searching of this section and others in Great Britain has failed to find any
 210 ammonites lower in the succession despite the recent discovery of *Neophyllites* in the White Lias (upper
 211 Lilstock Formation) of South Wales (Hodges, 2021) and an indeterminate psiloceratid in the Cotham
 212 Member of Gloucestershire (Donovan et al., 1989, Hodges 2021).

213 At Waterloo Bay crushed examples of *Psiloceras erugatum* (Phillips), are common in the upper part of Bed
 214 24 and base of Bed 25 (Simms and Jeram, 2007). Above this, beds 25 to 27 are dominated by the genus
 215 *Neophyllites*, with *N. imitans* Lange (Hn3-*imitans* Biohorizon of Bloos and Page, 2000) and *N. antecedens*
 216 Lange (Hn4-*antecedens* Biohorizon) in beds 26 and 27. Some, from near the top of Bed 26 and from Bed 27,
 217 have weakly developed ribbing on inner whorls and may be *Neophyllites ex gr. becki* (Schmidt) (Simms and
 218 Jeram, 2007).

219 *Psiloceras planorbis* is abundant in beds 28 to 33b, with the earliest examples occur 4 cm above the base of
 220 Bed 28. *Psiloceras sampsoni* (Portlock) occurs slightly higher in the Planorbis Subzone (Hn8-*sampsoni*
 221 Biohorizon) (Bloos and Page, 2000; Page, in Simms et al., 2004) (Simms and Jeram, 2007). Weakly plicate
 222 ammonites, assignable to *Psiloceras plicatulum* (Hn7-*plicatulum* Biohorizon), appear towards the top of Bed
 223 28b and persist through almost to the top of Bed 33e (Simms and Jeram, 2007). A succession of *Caloceras*
 224 faunas can be recognised in the succeeding Johnstoni Subzone at Waterloo Bay and the genus is represented
 225 by material in excellent preservation from here and, *ex situ*, from other sites in Northern Ireland (Figs 4 and
 226 5).

4.2 Cloghan Point, Whitehead

227 Cloghan Point lies on the north shore of Belfast Lough, 1 km south-west of the town of Whitehead and
 228 immediately north-east of the White Harbour (Fig. 1) (54° 44' 34" N, 5° 43' 4" W; Irish Grid Ref. J 470 907).
 229 A continuous, albeit faulted, section is exposed in a low cliff and adjacent intertidal foreshore from near the
 230 top of the Mercia Mudstone Group to the base of the Lias Group (Fig. 6a–c). The Cotham Member, briefly
 231 described in Simms (2007), is well exposed in the cliff with the Westbury Formation and uppermost beds of
 232 the Mercia Mudstone Group seen on the shore north-east of the slipway and the Langport Member to the
 233 south-west (Figs 6d–f). The Westbury Formation – Cotham Member boundary often is obscured by shingle
 234 (Fig. 6c). Green-grey conchoidally-weathering siltstones beneath the Westbury Formation here are
 235 lithologically identical to the underlying red Mercia Mudstone Group and lack the obvious bedding apparent

236 at Waterloo Bay, suggesting that the Collin Glen Formation here may have been eroded and the green-grey
237 siltstone merely represents a secondary reduction zone beneath the Westbury Formation.

238 The outcrop is cut by NNW–SSE and WNW–ESE faults, with vertical throws of 1–5 m. Bed thickness
239 variations and minor slumping at the tops of calcareous siltstone beds in the upper Westbury Formation
240 suggest synsedimentary fault movement prior to shallow burial cementation (see Macquaker, 1999). Wave-
241 rippled sandstones up to about 0.5 m thick, with siltstone and mudstone partings, occupy the lowest Cotham
242 Member. The unfossiliferous sandstones contain intraclasts of Westbury Formation mudstone that become
243 more common towards the faults, where soft-sediment deformation also is more intense (Fig. 6d).

244 Succeeding beds are mudstone-dominated, with subordinate lenticular/wavy-bedded grey siltstones. The
245 chocolate-brown to red-brown mudstones show regular lamination, with each mudstone lamina (mm to cm)
246 separated from the next by a silt parting <1 mm thick; these are the ‘striped measures’ of Ivimey-Cook
247 (1975). Small *Isocyprina* and *Protocardia* occur sparsely at some levels, with the conchostracan *Euestheria*
248 *minuta* (Zieten) present in the upper half of the brown mudstones. Bioturbation and trace fossils are largely
249 absent, with only *Lockeia* recorded. Soft-sediment deformation occurs throughout the red-brown mudstones,
250 increasing in intensity towards a fault (Fault B in Figure 6b, f). Its upper limit coincides with a change from
251 red-brown to grey mudstones and the highest deformed bed is truncated by an impersistent green-grey
252 lenticular sandstone, up to 0.1 m thick, with low-angle hummocky cross stratification, small flute casts and
253 linear tool marks on its base.

254 The succeeding upper Cotham Member comprises ~1.5 m of grey laminated mudstone with thin cross-
255 laminated sandstone/siltstone lenses in the lower part, succeeded by 2 m of laminated mudstone and marl
256 interbedded with eight cream-weathering micritic limestones up to 16 cm thick (Fig. 6a, c). Most limestones
257 are laminated but contain thin stromatolitic crusts with scours and laminae of reworked stromatolitic debris
258 and silt, with a more substantial stromatolite bed up to 4 cm thick developed at 0.4 m below the top of the
259 limestone series. The macrofauna comprises occasional microgastropods, juvenile bivalves (*?Isocyprina* sp.),
260 fish scales and a single bedding plane of *Euestheria* fragments in a laminated limestone one metre below the
261 top. Microfossils recovered from the limestones include the euryhaline ostracod *Darwinula* sp., the aquatic
262 liverwort *Naiadita* and diverse insect remains. Chironomid midges are especially abundant and represented
263 by all stadia from eggs to adults, with larval and adult head capsules extremely abundant in some samples
264 but absent in others and further investigation of the insect remains from this interval is required.

265 The highest limestone in the cliff is 0.25 m thick and is more massive and argillaceous than those below. It
266 lacks obvious sedimentary structures and grades into grey calcareous mudstone below and dark grey shaley
267 mudstone above, the latter probably equivalent to Bed 9 at Waterloo Bay. The marine bivalve *Protocardia* is
268 present in all three units. The base of the Langport Member is placed immediately beneath this dark
269 mudstone which, on the shore south of the slipway, is succeeded by half metre of dark grey mudstones (Fig.
270 4b), with occasional bivalves and a further >3 m of alternating siltstone and mudstone. Bivalves, particularly
271 *Protocardia* and *Liostrea*, occur in the burrow-mottled lower 2 m, with *Thalassinoides* and *Diplocraterion*
272 burrows abundant in the upper part. Micaceous siltstone and silty mudstone alternations dominate the next

273 metre, with bivalves confined largely to convex-up shell pavements on top of some siltstone beds. Dark grey,
274 shaley mudstone above a hard calcareous and micaceous siltstone, 0.2 m thick, is taken as the base of the
275 Waterloo Mudstone Formation here and probably correlates with Bed 14 at Waterloo Bay. A temporary
276 excavation a little further up the slope exposed shaley mudstones with crushed *Neophyllites* of the Planorbis
277 Subzone.

4.3 Cloghfin Port, Islandmagee

278 Cloghfin Port (54° 46' 29" N, 5° 41' 39" W; Irish Grid Ref. J 484 943) lies at the southern end of the
279 Islandmagee peninsula, 2.4 km NNW of Whitehead (Figs 1, 7). The foreshore outcrop dips at <10° to the
280 south-west and is truncated to the south by a NW–SE fault that downthrows Cretaceous strata (Hibernian
281 Greensands Formation) to the south. As at Cloghan Point, 3.7 km to the south-east, two sets of minor faults
282 cutting the Triassic have NNW–SSE and WNW–ESE trends that are repeated by intense minor fracturing,
283 down to mm-scale, in Westbury Formation sandstone beds adjacent to some faults (Fig. 7), but they are not
284 evident in the overlying Cretaceous cover. This soft-sediment and semi-brittle deformation adjacent to faults
285 indicates a discrete phase of seismicity during deposition of the upper Westbury Formation, prior to that
286 evident in the succeeding Cotham Member. Around 2 m of contorted grey and light brown coloured
287 mudstone and silty mudstone of the lower Cotham Member are exposed above a thin basal sandstone, also
288 strongly contorted. The upper Cotham Member is poorly exposed but includes undeformed pale grey
289 mudstones with silt laminae and convex-up shell pavements of *Protocardia* and several limestone beds
290 similar to those at Cloghan Point (Fig. 8). As at Cloghan Point green-grey conchoidally-weathering siltstones
291 beneath the Westbury Formation here are lithologically identical to typical red Mercia Mudstone Group from
292 which they are separated by a transitional ‘mottled zone’. It suggests that here too, as at Cloghan Point, the
293 Collin Glen Formation may be missing.

294 The main exposure of the Westbury Formation here resembles a shallow syncline with its eastern side
295 bounded by a NNW–SSE fault. Sandstone beds in the lower part of the Westbury Formation thicken and
296 merge towards the centre of this ‘syncline’, but small drag folds in mudstones adjacent to the fault suggest
297 that this ‘syncline’ actually represents enhanced sediment accumulation within a small graben or half-graben.
298 Higher in the Westbury Formation several fine-sandstone/siltstone beds and mudstone partings form erosion-
299 resistant ledges. The lowest of these (Bed L, Fig. 7), with regular repetitions of 0.5–1.0 cm thick planar
300 siltstone laminae topped with convex-up shell pavements and sand or mudstone partings, forms a useful
301 marker horizon at outcrop and in boreholes throughout the region (Boomer et al. 2020). Succeeding
302 siltstones vary in number and thickness, perhaps reflecting synsedimentary fault movement. They are usually
303 bioturbated in their upper part and commonly contain small slump structures.

304 Several minor faults appear to have propagated to the sediment surface at or near the end of Westbury
305 Formation deposition to create an irregular topography that was subsequently eroded. Consequently, the
306 Cotham Member basal sandstone rests on different stratigraphic levels within the Westbury Formation across
307 the outcrop (Fig. 7) yet it is relatively uniform in thickness and not offset by these faults. The highest part of

308 the Westbury Formation seen here (Fig. 7, sections 4 and 5) comprises contorted ‘pinstriped’ mudstones with
 309 very thin black, white and grey laminae, as at Cloghfin Port, indicating that the full thickness of the
 310 Westbury Formation is locally represented here. This ‘pinstriped’ lithofacies, unique within the Westbury
 311 Formation, may reflect background sedimentation of pale mud alternating with erosive episodes that released
 312 darker mudstone from nearby fault blocks.

313 Westbury Formation mudstones are intensely disturbed by soft-sediment deformation or liquefaction
 314 adjacent to the NNW-SSE trending fault, with thin sandstone stringers contorted or completely disrupted into
 315 irregular patches of sand. Sandstone beds more than 1 cm thick are largely intact but show brittle
 316 deformation, with two sets of fracture orientations matching those seen at larger scales across the outcrop. It
 317 suggests at least partial cementation by the time of their deformation, yet liquefaction of the enclosing
 318 mudstone suggests a shallow burial depth of just a few metres. Deformation appears to be related directly to
 319 movement on the NNW–SSE fault simultaneous with activity on the WNW–ESE faults.

4.4 *The Gobbins, Islandmagee*

320 A composite succession from the upper Cotham Member through into the Johnstoni Subzone of the
 321 Waterloo Mudstone Formation (Lias Group), mostly with a dip of about 10–15° NW, is patchily exposed on
 322 the shore along the landslipped eastern side of Islandmagee, about one kilometre south of The Gobbins and 4
 323 km NNW of Whitehead, (54° 47' 53" N, 5° 41' 29" W; Irish Grid Ref. J 485 969) (Fig. 1). These exposures,
 324 although not previously described, are significant because all biohorizons of the Planorbis Subzone and basal
 325 Johnstoni Subzone are present in mudstones that have not been thermally metamorphosed. The northern end
 326 of the outcrop is also the source of the only dinosaur remains yet found in Ireland (Simms et al., 2020). The
 327 exposures are described here from south to north and the succession summarised as a composite log and
 328 correlated with the other exposures in Figure 8.

329 In the most southerly exposure, Section 1 (54° 47' 31"N, 5° 41' 33" W; Irish Grid Ref. J 4845 9622), ~2 m of
 330 light grey calcareous mudstone and shale, with thin shelly bands containing abundant *N. antecessens*, are
 331 exposed at the top of the beach. These beds lie above 0.3 m of very shelly calcareous mudstone, its top
 332 covered with crushed *Neophyllites imitans*. This interval correlates with beds 25–27 at Waterloo Bay. *Ex-situ*
 333 carbonate nodules containing *P. erugatum* have been found on the shore nearby, while slipped material
 334 nearby includes blocks of dark shale containing crushed *P. planorbis*. A few metres higher and to the north,
 335 *P. sampsoni* and *P. plicatulum* have been found in situ, with *Caloceras* sp. recovered from a mudflow higher
 336 on the bank.

337 Landslip obscures the outcrop until Section 2 is reached (54° 47' 35.5" N, 5° 41' 29.4" W; Irish Grid Ref. J
 338 4851 9635), where the ‘pre-planorbis’ beds are exposed for about 40 m along the intertidal area. Two hard
 339 limestone bands exposed near low water mark, each 5–6 cm thick and with contorted ‘clasts’ of mudstone
 340 and discontinuous mudstone partings, correlate with shelly limestone beds near the base of the Waterloo
 341 Mudstone Formation at Waterloo Bay (Bed 18). Softer contiguous beds are obscured by shingle, but ~0.6 m

342 of finely interbedded siltstone and micaceous mudstone, with 3 or 4 thin impersistent limestone ribs towards
 343 the top, are exposed further down-dip and probably correlate with Bed 21 at Waterloo Bay. It is succeeded
 344 by ~0.7 m of dark grey micaceous mudstone, calcareous in the top 0.2 m. Above this lies 3 m of paler
 345 micaceous mudstone with bands of *Liostrea* in its lower part and an impersistent lenticular shelly limestone,
 346 up to 8 cm thick, at its top. Abundant thick-shelled *Cardinia ovalis* (Stutchbury) allow tentative correlation
 347 of this limestone with Bed 23 at the Waterloo Bay section. Higher beds are represented by a small, isolated
 348 exposure beneath the cliff where ~1 m of grey calcareous mudstone, with two 0.25 m thick shelly beds, has
 349 yielded indeterminate ammonite fragments suggesting they may correlate with beds 24 and 25 at Waterloo
 350 Bay.

351 Section 3, further down-dip (54° 47' 37.4" N, 5° 41' 29.9" W; Irish Grid Ref. J 4850 9641), a section exposes
 352 more than 6 m of Waterloo Mudstone Formation along some 20 m of the upper foreshore and adjacent low
 353 cliff. The lower part of the succession is dominated by dark shaley mudstones with subordinate calcareous
 354 mudstones and pyritic bands. Higher beds tend to be paler mudstones and include several orange-weathering
 355 siltstone bands with abundant *Chondrites* burrows. *Psiloceras planorbis* occurs in the lowest beds,
 356 succeeded by *P. sampsoni* (1.0 m above base), *P. plicatulum* (1.5–2.5 m above base), *Caloceras cf. johnstoni*
 357 (4.3 m above base) and *Caloceras* sp. indet. (4.9 m above base), with individual units here correlating with
 358 beds 28–34 at Waterloo Bay (Simms and Jeram 2007). A few metres below this exposure, in the intertidal
 359 zone, two small isolated outcrops each expose ~0.5 m of grey mudstone, with the stratigraphically higher
 360 containing crushed *Neophyllites ?antecedens* and the lower containing *Neophyllites* sp. fragments.

361 Section 4 (not shown on Figure 8) is located ~200 m south of the start of The Gobbins cliff path and north of
 362 a rotational slip that brings Ulster White Limestone Formation (Cretaceous, Chalk Group) down to beach
 363 level (54° 47' 53.9" N, 5° 41' 26.1" W; Irish Grid Ref. J 4855 9692). It exposes ~2 m of pale grey laminated
 364 mudstone with several cream-coloured limestones that clearly correlate with those in the upper Cotham
 365 Member, as seen at Waterloo Bay and Cloghan Point. The outcrop here dips to the south-west, unlike those
 366 further to the south that dip north-westwards, suggesting that they may lie either side of a synclinal axis
 367 orientated NE–SW.

5. Triassic–Jurassic boundary events in Northern Ireland

5.1. Carbon stable-isotope excursions

368 The succession at Waterloo Bay was sampled for geochemical analysis at 10 cm intervals from 0.5 m below
 369 the ‘mud-cracked’ horizon of the Cotham Member (0 m in Fig. 3) up to the first frequent occurrence of *P.*
 370 *plicatulum* at the top of Bed 28b (159 samples) (Fig. 3). This sampling resolution is at least twice that for the
 371 same interval in the nearby Carnduff-2 borehole (Boomer et al., 2020) and substantially greater than that for
 372 St Audrie’s Bay (Hesselbo et al., 2002). Lower strata in the Penarth Group were not sampled because of
 373 more intense thermal alteration and/or soft-sediment deformation. Geochemical analyses were undertaken at
 374 the University of Oxford. Bulk organic $\delta^{13}\text{C}$ values (‰), calibrated relative to the Vienna-Pee Dee Belemnite

375 (VPDB) standard. Total organic carbon (TOC) percentage and % CaCO₃ were measured in samples and are
376 shown in Figure 3 beside the isotope data.

377 The carbon stable-isotope curve shows a broad pattern of positive and negative trends comparable with those
378 identified from south-west England (Hesselbo et al., 2002, Clémence et al., 2010) and the Carnduff-2
379 borehole (Boomer et al., 2020). The expanded stratigraphy and greater sample density at Waterloo Bay
380 produced a curve where the ‘excursions’ appear more gradual and less pronounced than those for south-west
381 England, but with additional minor fluctuations that are not resolvable in these more coarsely sampled
382 successions. A drop in $\delta^{13}\text{C}$ values around Bed 10 at Waterloo Bay can be correlated with the top of the
383 ‘initial’ negative CIE of Hesselbo et al. (2002) and the interval between beds 2 and 10 shows four
384 oscillations in $\delta^{13}\text{C}$ of $\sim 2\text{--}3\%$. Similar oscillations are seen in Hungary (Pálffy et al., 2007) and Morocco
385 (Dal Corso et al., 2014) and also in the nearby core from Carnduff-2 (Boomer et al., 2020, figure 10B) but
386 they are not evident in the coarsely sampled curves of north Somerset. A return to more positive values
387 precedes another negative excursion, around beds 21 and 22a, which corresponds to the start of the ‘main’
388 negative CIE (Fig. 3). The negative trend in $\delta^{13}\text{C}$ is mirrored by a corresponding slight positive trend in TOC
389 (Fig. 3).

390 It has been shown in sections from Denmark that sharp negative spikes in the carbon stable-isotope record
391 correspond to peaks in algal sphaeromorph abundance (Lindström et al., 2012) and Bonis et al. (2010)
392 argued that the palynological record at St Audrie’s Bay reflected the influence of orbitally forced climate
393 cyclicity on the input and composition of organic matter into the system, and there is a striking relationship
394 between isotope values and palynological composition of samples from Germany (van de Schootbrugge et
395 al., 2013). However, in the absence of palynological records from Waterloo Bay it is difficult to explore
396 these relationships. Palynological samples were collected by Simms and Jeram (2007) but they were too
397 thermally altered to be useful and only sparse palynological records have been published from the nearby
398 Larne-1 Borehole (Warrington and Harland, 1975). Further palynological sampling and analysis from the
399 Carnduff-1 Borehole, <3 km distance (Boomer et al., 2020) could be carried out explore the relationships
400 between carbon isotope excursions and palynology in the Larne Basin, where the stratigraphy is relatively
401 expanded. Some of the minor variations in the Waterloo Bay stable-isotope record may have similar climate
402 cycle causes, although Fox et al. (2020) have claimed that the ‘initial’ CIE is a consequence of ecological
403 and biotic changes linked to marine to non-marine changes, associated with eustatic sea-fall, rather than
404 reflecting input of light volcanogenic carbon. Implications of the Waterloo Bay stable-isotope record for
405 wider correlation are discussed in sections 6.1 and 6.2.

406

407 5.2. *Depositional setting*

408 Marine indicators in parts of the Collin Glen Formation of the Carnduff boreholes (Boomer et al., 2020)
409 record the initial stages of a diachronous onlap associated with the basal Rhaetian transgression (Mayall,
410 1981; Hesselbo et al. 2002; Barth et al., 2018). The Westbury Formation was deposited in a relatively

411 shallow, storm influenced, offshore marine environment, with winnowing and re-suspension of mud perhaps
412 discouraging benthic colonization (Hesselbo et al. 2004, Barras and Twitchett, 2007). Six or seven
413 sedimentary cycles can be recognised in the studied sections in the Larne Basin, with sand/silt dominated
414 sediments alternating with mud. Synsedimentary fault control, similar to that seen at Cloghfin Port, may
415 have influenced the number and thickness of individual sandstone beds in the Westbury Formation and the
416 thickness of the unit across the basin. Although evidence for shallowing of facies in the upper Westbury
417 Formation is reported from southern Britain (Hesselbo et al., 2004) in Northern Ireland black pyritic shaley
418 mudstones persist to the top of the formation in most parts of the Larne Basin studied. The upper boundary
419 of the Westbury Formation however corresponds to a period of erosion, either through tectonic uplift or
420 eustatic sea-level fall and possibly post-deposition of the Westbury Formation, with pronounced erosion of
421 the formation top toward the margin of the Larne Basin. Soft sediment deformation in the lower Cotham
422 Member (Simms, 2007; Laborde-Casadaban et al., 2021), discussed in Section 6.3, also affected the upper
423 part of the Westbury Formation. It may have been linked with minor (metre-scale) tectonic uplift, but
424 renewed transgression above the soft sediment deformed beds and into the lower part of the Langport
425 Member is evident in all sections.

426 Silty mudrocks of the lower Cotham Member mark an abrupt change (Fig. 9a) from a relatively offshore
427 situation to very shallow water, with a scarcity of trace fossils or bioturbation and marine bivalves
428 suggesting rapid deposition and/or fluctuating salinity. No consistent fining- or coarsening-up pattern is seen
429 above the Cotham Member basal sandstone and individual units cannot be correlated easily between
430 outcrops. It is difficult to construct a facies model for the Cotham Member from the limited exposures
431 studied here, but flooding of the NW European epicontinental seaway and a subsequent regression, may have
432 produced a series of islands among shallow quasi-marine seaways over a vast area (e.g. see figure 1 in
433 Lindström et al., 2015). Tidal currents, influenced by the location and disposition of land masses and eustatic
434 effects (Reynaud and Dalrymple, 2012), probably were complex and locally variable. As such, the Cotham
435 Member in the Larne Basin may represent a continuously changing mixed system, at times showing
436 sedimentological features of estuarine, tidal flat, shallow shoreface, or lagoonal deposits, but without the
437 clear facies associations characteristic of any of them. For the most part, the heterolithic facies of the Lower
438 Cotham Member exhibit features that indicate deposition on shallow subtidal flats. The lower Cotham
439 Member at Waterloo Bay has a higher content of fine sand and silt than at Cloghan Point or Cloghfin Port,
440 suggesting a more offshore subtidal setting in which stronger tidal currents pushed mud further inshore. A
441 weak fining-up trend is discernible, perhaps a result of shoaling or shallowing due to eustatic sea-level fall
442 towards the ‘mud-cracked’ horizon. The succession appears to have been laid down under generally quiet
443 peritidal conditions, with frequent evidence of rhythmic bedding (Fig. 9c-d), channel erosion (Fig. 9c), and
444 ripples containing internal mudstone drapes (Fig. 9b). Scours are present at various levels above and below
445 the ‘mud-cracked’ surface, attesting to intermittent storm-related erosion, and a few thin sandstone beds
446 contain very low angle hummocky cross stratification. Other thin sandstone bodies are comprised of
447 unidirectional cross-stratified sandstone, with multiple reactivation surfaces.

448 Fox et al. (2020) have suggested that algal biomarkers from the upper part of the Cotham Member (across
449 the ‘initial’ CIE) at the St Audrie’s section indicate deposition within very shallow waters that received an
450 influx of fresh and brackish water due to a marked relative sea-level fall. They proposed that the drop in sea-
451 level could result from rising of hot asthenosphere that caused doming of the crust and uplift of the European
452 basins, or closure of marine gateways into the already restricted European basins, or eustatic sea-level drop
453 due to polar ice growth resulting from CAMP related SO₂ emissions. Sedimentation following an event such
454 as this would be less connected to eustatic change and more reliant on climate, water chemistry and facies
455 shoaling and progradation.

456 The ‘initial’ CIE in the Larne Basin starts immediately below the Cotham Member carbonates and peaks
457 immediately above it (Fig. 3), coinciding with a change in the marine flora from dinoflagellate-dominated in
458 the Westbury Formation and lower Cotham Member, to acritarch/prasinophyte-dominated assemblages
459 above in the Carnduff-1 Borehole (Boomer et al., 2020). In Northern Ireland, where the upper boundary of
460 the Cotham Member is somewhat gradational and the upper part of ‘initial’ CIE seems to extend into the
461 lower Langport Member, the return to more fully marine conditions may be better preserved or be more
462 expanded.

463 Minor shallowing in the early Langport Member coincides with the end of the ‘initial’ CIE while higher beds
464 show a gradual diversification of the marine fauna (Ivimey-Cook, 1975; Simms and Jeram, 2007) and
465 development of lenticular bedded siltstone and silty mudstone indicative of slightly deeper water
466 sedimentation, perhaps as sub-littoral, storm-generated sheet deposits. There is no evidence for erosion at the
467 top of the Langport Member here and higher parts of the member elsewhere in SE County Antrim suggest
468 relative environmental stability compared with beds above and below, as indicated by minimal variation in
469 % organic carbon or % carbonate and relatively little fluctuation in the $\delta^{13}\text{C}$ record (Fig. 3).

470 The base of the Waterloo Mudstone Formation marks a flooding event (Fig. 10), with fully-marine offshore
471 conditions rapidly established followed by transgression to an early Planorbis Zone highstand, before a
472 eustatic fall towards the top of that zone (Simms and Jeram, 2007; Barth et al., 2018). This may have been
473 associated with hypoxia below storm wave base and corresponds to the most positive $\delta^{13}\text{C}$ values
474 immediately prior to the onset of the ‘main’ carbon stable-isotope excursion and high TOC (Figs 3, 10),
475 similar to the excursion at the lower/upper Cotham Member junction.

476

5.3. Seismic events

477 The intense soft sediment deformation in the lower Cotham Member at Waterloo Bay and Cloghan Point was
478 initially ascribed to the effects of a single large magnitude seismic event (Simms, 2003, 2007), but similar
479 deformation in the upper Westbury Formation testifies to several episodes of pre-Cotham Member seismic
480 activity (Fig. 10) (see also Laborde-Casadaban et al., 2021; Lindström et al., 2015). Seismic shock need not
481 be the only cause of soft-sediment deformation and it should be acknowledged that the typical Cotham
482 Member mudstone-siltstone facies (Fig. 9) would be particularly susceptible, but the uniformly low gradients

483 of the Rhaetian environment across much of the UK and a lack of comparable deformation in contiguous
484 strata of similar facies, suggests that other mechanisms, such as gravity sliding, can be discounted in this
485 instance.

486 The sandstone at the base of the Cotham Member is undeformed in some places, such as Cloghan Point, but
487 at Waterloo Bay it is highly contorted, locally intrudes up to 0.15 m into the underlying Westbury Formation,
488 and is overlain by highly-contorted sandstone-mudstone interbeds (Fig. 9a). The overlying Cotham Member
489 contains a strongly deformed horizon, which exhibits intermittent recumbent folding where alternations of
490 silt and clay make it visible, but deformation occurs within the more argillaceous intervals also (Laborde-
491 Casadaban et al., 2021). Supposed tsunami 'rip-up clasts' towards the top of the most intensely deformed
492 beds at Larne (Simms 2003, 2007) probably represent 'pseudo-nodules' of more-cohesive sediment that
493 failed to liquefy under the lower pore pressures at the top of the seismite. Similar features have been
494 recorded from Rhaetian strata by Lindström et al. (2015, figure 2D).

495 Overlying the deformation a 'mud-cracked' surface at Waterloo Bay (Fig. 11a–c) has been interpreted as
496 evidence for emergence (Simms, 2003, 2007) but these cracks lack the 90° T-junctions characteristic of
497 desiccation cracks (Goehring, 2013), with intersection angles for many of less than 45° and cross-cutting
498 relationships that may involve up to four generations of cracks. Most are less than 10 cm deep, yet some
499 narrow cracks run straight for more than 1.5 m, whilst spindle-shaped cracks may be curved, taper rapidly in
500 either direction, or lack intersections (Fig. 11a). In vertical section most are at low angles to the bedding,
501 ptygmatic and usually without sharp sides. They often change angle abruptly and/or branch (Figs 11b-c),
502 commonly show sub-surface crack intersections and some appear to have been secondarily deformed by
503 horizontal compression and shear. Together these features are suggestive of subaqueous sedimentary, or
504 synaeresis, cracks (*sensu* McMahon et al. 2016) rather than subaerial desiccation cracks. Synaeresis cracks
505 require a cohesive substrate susceptible to brittle deformation (McMahon et al., 2016) and may have been
506 seismically induced (Pratt, 1998), although salinity changes or gas formation have been proposed as
507 alternative mechanisms (e.g. McMahon et al., 2016; Siebach et al., 2014). The Waterloo Bay cracks were
508 clearly initiated at or near the sediment surface, perhaps implying brief emergence and drying to confer a
509 degree of cohesiveness on otherwise unconsolidated mud, but they are overlain by a thin lenticular sandstone
510 with interference ripples that suggest shallow subtidal or intertidal deposition. Although this cracked surface
511 is unique within a 6 m succession of similar facies, it seems probable that the 'mud-cracked' surface and at
512 least one of the underlying deformed intervals may stem from the same seismic event. Correlation of these
513 surfaces within the UK (Mayall, 1983; Simms, 2007; Laborde-Casadaban, 2021), and a similar synaeresis-
514 cracked surface in the Schandelah-1 core of the Germanic Basin (Lindström et al., 2015, 2017), is indicated
515 by their position immediately below the start of the 'initial' CIE (Fig. 3). Whether these features relate to a
516 series of different seismic events across separate basins that due to sediment characteristics or water column
517 depth were expressed in the same way or one single seismic event remains unclear.

518 The 30 cm thick bed of wave-rippled sandstone/mudstone heterolith that overlies the 'mud-cracked' horizon
519 undulates gently (wavelength of ~1 m and amplitude of ~0.05 m) but is cut by narrow sub-vertical fracture

520 zones, resembling kink bands, that are associated with contorted bedding (see Moretti and van Loon 2014,
 521 figure 2, for a modern example). These deformation zones cannot be traced into contiguous beds and perhaps
 522 formed through hydrofracturing. Its presence above the ‘mud-cracked’ horizon suggests further seismic
 523 activity in the upper Cotham Member.

6. Discussion

6.1 Correlation of the Waterloo Bay section with Somerset (St Audrie’s and Doniford bays)

524 Correlation has been attempted many times between the St Audrie’s Bay record and the GSSP in Kuhjoch,
 525 Austria and there still remains some uncertainty as to the precise level of the TJB in the GB curves (Wignall
 526 and Atkinson, 2020). Correlating the succession in Northern Ireland with that in North Somerset, more than
 527 400 km to the south-east, may assist correlation with the Austrian GSSP 1600 km to the south-east of
 528 Waterloo Bay, Larne (Fig. 12). Northern Ireland and Somerset share some lithostratigraphic events which, if
 529 synchronous rather than diachronous, may aid correlation between those sites and with the GSSP. The
 530 carbon isotope profile from Waterloo Bay offers significantly finer resolution than published data from
 531 south-west Britain and corroborates the first-order trends seen in other curves from the UK.

532 The Westbury Formation is broadly similar across the UK, with its top marked by a relative sea-level fall
 533 presumed to be a regional event. The succeeding Cotham Member also is fairly uniform in lithology and
 534 fauna across the UK and includes an apparently synchronous period of seismically-induced soft-sediment
 535 deformation in its lower part and stromatolitic horizons both in south-west Britain and in Northern Ireland.
 536 The ‘initial’ CIE of Hesselbo et al. (2002) lies above the ‘mud-cracked’ horizon found in many parts of the
 537 UK, supporting a correlation, but the finer resolution and expanded stratigraphy in County Antrim also
 538 suggest that the upper part of the ‘initial’ CIE may be attenuated or truncated in south-west Britain, where
 539 the top of the Cotham Member is represented by the locally developed stromatolitic Cotham Marble
 540 (Hamilton, 1961), a bed that is in some locations bored and eroded at the base of the Langport Member
 541 (Richardson, 1911; Swift, 1995; Benton et al. 2002). In County Antrim the lower part of the excursion
 542 coincides with microbially laminated limestones, claystones and a thin stromatolitic limestone, that together
 543 are perhaps broadly equivalent to the Cotham Marble. The peak of the excursion at Waterloo Bay lies in
 544 higher beds that can be correlated lithologically with the lower Langport Member of the Bristol Channel
 545 Basin. Boomer et al. (2020) recorded the peak of the ‘initial’ CIE near the top of the Cotham Member in the
 546 Carnduff-2 Borehole, sited just 3 km south west of the Waterloo Bay section.

547 As a lithostratigraphic unit the Langport Member may not be isochronous across the UK. Comparing $\delta^{13}\text{C}$
 548 data from the key sites of Lavernock Point in south Wales, Pinhay Bay in Devon, (Korte et al., 2009, figure
 549 6) and St. Audrie’s Bay in Somerset (Hesselbo et al., 2002, 2004) suggests that much of the Langport
 550 Member at Lavernock Point and Pinhay Bay may correlate with part of the basal Blue Lias Formation at St.
 551 Audrie’s Bay (Figs 10 and 12). Cyclostratigraphy also suggests that the base of the Blue Lias Formation may
 552 be diachronous (Weedon et al. 2018, figure 14). Similarly, if a minor (1.5‰) negative shift in $\delta^{13}\text{C}$ at 1.8 m

553 above the base of the Langport Member at Waterloo Bay (base of Bed 13, Fig. 3) does correlate with the
554 minor negative shift at the base of the Blue Lias Formation in St Audrie's and Doniford bays (marked 'C' on
555 Fig. 12), then the base of the Blue Lias Formation at St Audrie's Bay may be older than elsewhere. Hence
556 the upper Langport Member at Lavernock Point and Pinhay Bay, and beds 13 and 14 of the Langport
557 Member at Waterloo Bay, may be lateral, possibly shallower water, equivalents of the basal Blue Lias
558 Formation on the North Somerset coast. If correct, then this implies that the organic-rich mudrock that
559 commonly lies at the base of the Lias Group in the UK may also be diachronous, implying that anoxia
560 developed at different times depending on water depth or sedimentation rates (Hesselbo et al., 2004; Korte et
561 al., 2009).

562 Above the base of the Lias Group the carbon isotope curves at St Audrie's and Doniford bays are near
563 identical while that of Waterloo Bay is broadly similar but shows more detail and irregularity due to the
564 higher sampling resolution (Fig. 12). In fact the expanded stratigraphy and greater sampling resolution of the
565 isotope curve at Waterloo Bay presents its own issues with regard to correlating peaks against those of less
566 highly resolved records. Comparison can also be made with the curve from the Carnduff-2 borehole
567 (Boomer et al. (2020), <3 km from the Waterloo Bay section, which although of lower resolution offers
568 greater coverage of the stratigraphy by sampling the entire Penarth Group and extending to higher levels in
569 the Lias Group.

570 A gradual decline at the start of the 'main' CIE in all four curves steepens towards the first negative trough
571 beyond which the first minor positive peak (Peak A in Figure 12), evident in the Waterloo Bay and Doniford
572 Bay curves, but more subtle in the Waterloo Bay curve and appears to be shown in the Carnduff-2 curve
573 (Boomer et al. 2020, figure 10). The next positive peak seen in the Doniford Bay curve may represent an
574 average of three small peaks in the Waterloo Bay curve (B in Fig. 12), with *P. erugatum* in the succeeding
575 negative trough at both sites lending support to this correlation. Neither peak nor trough can be resolved in
576 the more coarsely sampled and condensed succession at St Audrie's Bay although *P. erugatum* is present at
577 this level and it is not observed in the coarsely sampled interval in the Carnduff-2 data (Boomer et al., 2020).
578 Minor positive peaks, corresponding to the first appearances of *P. planorbis* and *P. plicatulum*, can also be
579 matched between Waterloo Bay and the two curves in Somerset (Fig. 12), although the stratigraphic
580 occurrence of these ammonites is the main factor in verifying this correlation. It should be noted that in
581 Figure 12 the blue shading used to indicate the 'initial' and 'main' carbon stable-isotope excursions *sensu*
582 Hesselbo et al. (2002) marks the primary negative trend of each excursion only and not the ensuing positive
583 trend. Hesselbo et al. (2002) did not define an upper limit to the 'main' CIE and so, for the purposes of
584 discussion comparison with other carbon isotope records, the 'main' CIE is restricted here to the rapid 3.5–
585 4.0‰ decline in $\delta^{13}\text{C}$ that follows the positive excursion seen at the base of the Blue Lias Formation at St
586 Audrie's Bay (Fig. 12). At Waterloo Bay and the two sites in Somerset the rapid $\delta^{13}\text{C}$ decline is interrupted
587 near its top by a minor positive excursion (peak A in Fig. 12) above which $\delta^{13}\text{C}$ values decline to a minimum
588 that can define the top of the 'main' negative CIE and above which there is a slight positive trend up to the
589 first appearance of *P. planorbis*. This trend lies within a sample gap in the Carnduff-2 record, but its likely

590 position constrained by peak negative values slightly shallower than the base of the *plicatulum* Biohorizon at
 591 345 m depth (Boomer et al., 2020).

6.2 The Triassic–Jurassic boundary in Northern Ireland

592 The Triassic–Jurassic boundary (TJB) has been defined by the first occurrence (FO) of *Psiloceras spelae*
 593 *tyrolicum* Hillebrandt and Krystyn, in the GSSP at Kuhjoch, Eiberg Basin of Austria (Hillebrandt et al.,
 594 2013). This ammonite taxon has not been found in NW Europe nor can it be readily correlated with any of
 595 the early Hettangian ammonite biohorizons recognized in the region. In NW Europe, the base of the
 596 Planorbis Zone is drawn below the *imitans* Biohorizon (Hn3) (based on *N. imitans*) and the underlying strata,
 597 that includes the *erugatum* Biohorizon (Hn2) (based on *P. erugatum*) down to the base of the Hettangian
 598 Stage, now assigned to the Tilmanni Zone (Page, 2010; Hillebrandt et al., 2013; Weedon et al., 2019). Only
 599 three ammonites have been found below the Hn2 Biohorizon in the UK (Opazo and Page, 2021), with all of
 600 Late Triassic age. A single indeterminate psiloceratid, reportedly from the top of the Westbury Formation in
 601 Gloucestershire (Donovan et al., 1989), is actually from near the base of the Cotham Member (Hodges,
 602 2021). More recently two ammonite specimens described as *Neophyllites lavernockensis* Hodges have been
 603 found in the White Lias (Langport Member) of South Wales (Hodges, 2021).

604 With such a dearth of biostratigraphically useful ammonite or other macrofossil taxa, low abundance and/or
 605 poor recovery of calcareous microfossils and lack of diagnostic marine marker palynomorphs in this interval;
 606 in Northern Ireland (Boomer, et al., 2020) carbon isotope excursions offer perhaps the best potential for
 607 correlating the TJB to this region, but current resolution of the isotope data allows for more than one possible
 608 correlation.

609 The ammonite-defined Triassic–Jurassic boundary in the Eiberg Basin, Austria has been correlated with
 610 three different levels in the St Audrie’s Bay succession, each of which in turn can be correlated with the
 611 more finely resolved Waterloo Bay carbon stable-isotope curve (Fig. 12).

612 The inflection in the ‘main’ CIE, shown as Level 1 in Figure 12, offers one possible correlation to the TJB
 613 level in the GSSP (Kürschner 2007; Hillebrandt et al., 2007) and has been accepted in several subsequent
 614 publications (e.g. Simms and Jeram, 2007; Ruhl et al., 2009, Whiteside et al., 2010; Ruhl and Kürschner,
 615 2011; Steinthorsdottir et al., 2011; Jaraula et al., 2013; Hüsing et al., 2014; Dal Corso et al., 2014; Kent et
 616 al., 2017). It places the TJB above the start of the 4‰ ‘main’ negative CIE at St Audrie’s Bay (Hesselbo et
 617 al., 2002) but others (Guex et al., 2004; Clémence et al., 2010; Bartolini et al., 2012) have correlated the first
 618 occurrence of *P. spelae* in Nevada with a level below the start of the ‘main’ CIE. Correlating the TJB to
 619 Level 1 would, therefore, imply that the first occurrence of *P. spelae* in North America might be earlier than
 620 that of *P. spelae tyrolicum* in Austria (Ruhl et al., 2009; Korte and Kozur, 2011). However, since *P. spelae*
 621 occurs only within restricted stratigraphic intervals separated from other psiloceratid occurrences by strata
 622 barren of ammonites, this apparent time gap may be an artefact of preservation.

623 Two biotic events of potential correlative value between Level 1 and the TJB are the first occurrence of
624 *Isocrinus angulatus* 1 m above the base of Bed 22a at Waterloo Bay (Simms and Jeram, 2007; Hillebrandt et
625 al., 2013; Simms, 2021) and the flood appearance (one sample showing a ten-fold increase in abundance) of
626 the robertininid foraminifera *Reinholdella? planiconvexa* (Fuchs) in the Carnduff-1 Borehole at a level
627 which correlates to Bed 22b at Waterloo Bay (Boomer et al., 2020). This flood of foraminifera is an event
628 that can be widely recognised, including in the Lough Foyle Basin of Northern Ireland (Raine et al., 2021), at
629 Doniford Bay in Somerset (Clémence and Hart, 2013), and possibly also in Austria Hillebrandt et al., (2013),
630 although more work is required on the taxonomy of the UK examples. Although both events may have been
631 environmentally controlled, nevertheless, they maintain a remarkable relationship to each other and to the
632 carbon isotope stratigraphy (Fig. 12).

633 Correlation at Level 2 (Fig. 12) has been suggested by Ruhl and Kürschner (p. 193 and figs 18–19 in
634 Hillebrandt et al., 2013) who considered that the FO of *P. spelae* in the Austrian GSSP section lay within the
635 ‘main’ CIE. However, comparing data from the GSSP, St Audrie’s Bay and New York Canyon (Nevada)
636 offered an alternative interpretation (fig. 27 of Hillebrandt et al., 2013) and correlated the 4‰ negative
637 excursion above the ‘Schattwald Beds’ of the Tiefengraben Member with a minor 1.6‰ shift at the base of
638 the Blue Lias Formation in St. Audrie’s Bay (C in Fig. 12), rather than with the main 4‰ ‘main’ negative
639 excursion (see also Korte et al., 2009). The correlation is based on the assumption that *P. spelae tyrolicum* at
640 the GSSP and *P. spelae spelae* in the Nevada section are isochronous and the correlation has been adopted,
641 with minor variations, by recent authors (e.g. Percival et al., 2017; Korte et al., 2019; Ruhl et al. 2020).

642 The final option (Level 3 in Figure 12) for the TJB within the UK places the TJB within the ‘initial’ CIE
643 (Hesselbo et al., 2002) at St Audrie’s Bay (Lindström et al, 2017, 2019), based upon the argument that a
644 distinct 6‰ negative CIE at the junction of the Kössen and Kendelbach formations in the Northern
645 Calcareous Alps (Ruhl et al., 2009) was earlier than the ‘initial’ excursion at St Audrie’s Bay. This
646 interpretation could be supported by an abundance peak of the spore taxon *Polypodiisporites*
647 *polymicroforatus* (Orłowska- Zwolińska) below the ‘initial’ CIE in NW Europe, which has been correlated
648 with a similar peak above the Kössen–Kendelbach isotope excursion in the Eiberg Basin, Austria. This
649 would imply that the last appearance of the latest Triassic ammonites *Choristoceras marshi* Hauer and *C.*
650 *crickmayi* Tozer, marking the primary marine extinction level, correlates with a level in the Westbury
651 Formation of the UK rather than with the start of the ‘initial’ CIE at the lower/upper Cotham Member
652 boundary. This correlation was rejected by Korte et al. (2019) because it failed to consider other available
653 stratigraphic markers.

654 As suggested by Boomer et al. 2020, who looked at microfossil, palynology and carbon isotope records for
655 the Carnduff boreholes, if the ‘initial’ CIE at Carnduff and in the Kuhjoch section represent the same event,
656 then the Triassic–Jurassic boundary must be within the very highest part of the Langport Member or above it
657 (i.e. in the Waterloo Mudstone Formation). It must, therefore, lie between the top of the ‘initial’ CIE and the
658 first occurrence of ammonites, a 10–11 m interval in the cores. Palynological data would suggest it lies at the
659 very top of the Langport Member in the Carnduff cores, based on the first occurrence of *Cerebropollenites*

660 *thiergartii* (Level 2 in Figure 12) (Boomer et al. 2020). This point on the carbon isotope curve at Waterloo
661 Bay lies above a \sim 1–1.5‰ negative shift in the Langport Member, which appears to correlate with similar
662 shifts in the Doniford and St Audrie’s bay records that lie in the lower part of the Blue Lias Formation (point
663 C in Fig. 12). Unfortunately this shift was not identified in the Carnduff-2 Borehole record (Boomer et al.
664 2020).

665

666 *6.3 Atmospheric carbon dioxide concentration ($p\text{CO}_2$)*

667 Carbon dioxide concentrations, derived from stomatal index values of plant cuticle, have been reported from
668 the Larne Basin T–J succession (Fig. 10) and compared with data from East Greenland (Steinthorsdottir et
669 al., 2011). Cuticle samples of *Brachyphyllum*, a cheirolepidacean conifer that was the only morphotype
670 present at all sampled levels, were obtained from the sections described here at Cloghan Point, The Gobbins
671 and Cloghfin Port and are correlated with the Waterloo Bay section to compare with the carbon isotope
672 record documented here (Fig. 8). The primary trend suggests increasing $p\text{CO}_2$ from the Westbury Formation
673 through into the Planorbis Zone of the Waterloo Mudstone Formation (Fig. 10) and is evident in other cuticle
674 morphotypes in the Larne Basin and in East Greenland (Steinthorsdottir et al., 2011, 2018).

675 The Larne Basin data show that $p\text{CO}_2$ continued to rise, between WL2 and G3 to reach a peak around the G3
676 level (Steinthorsdottir et al., 2011, figure 5) that corresponds to the start of the ‘main’ CIE and the onset of
677 interpreted rapid relative sea-level rise in the Larne Basin (Fig. 10). Above the G3 level $p\text{CO}_2$ estimates from
678 different plant groups diverge. Conifer cuticle indicates no significant change but ginkgoalean and
679 bennettitalean cuticle suggest declining $p\text{CO}_2$ (Steinthorsdottir et al., 2011, figure 6). These differences
680 suggest that one or other plant groups may have been responding to drivers other than $p\text{CO}_2$ at that time. The
681 relatively low-resolution dataset of $p\text{CO}_2$ estimates from the Larne Basin can provide only an approximate
682 indication of $p\text{CO}_2$ change through the T–J interval and is unlikely to have sampled the maxima or minima,
683 nor does it allow resolution of the pulsed nature of $p\text{CO}_2$ change suggested by the data of Schaller et al.
684 (2011, 2012). Nevertheless, it does identify a significant rise in $p\text{CO}_2$ associated with the ‘initial’ CIE and
685 indicates that $p\text{CO}_2$ generally remained at elevated levels for some time. The $p\text{CO}_2$ proxy data indicate a
686 fairly sustained doubling of $p\text{CO}_2$ from Late Rhaetian background levels above the ‘initial’ CIE (Schaller et
687 al., 2011, 2012; Steinthorsdottir et al., 2011), suggesting a mean global temperature increase of \sim 2.5–5 °C
688 between the ‘initial’ CIE and the Planorbis Zone (e.g. Royer et al., 2007; Steinthorsdottir et al., 2011) and
689 perhaps linked to pulsed CO_2 emissions from the later phases of CAMP basalt eruptions.

690

691 *6.4 Seismic activity*

692 The soft sediment deformation seen in the Larne Basin is ascribed to seismic activity during the TJB interval
693 (Simms, 2003, 2007; Laborde-Casadaban et al., 2021). Widespread soft-sediment deformation through the
694 TJB interval in north-west Europe has in the past been ascribed to seismicity associated with rifting of the
695 proto-Atlantic (Swift, 1999; Hesselbo et al. 2002), associated with CAMP activity (e.g. Hallam and Wignall,

696 1999; Wignall and Bond, 2008; Lindström et al., 2015), or due to bolide impact (Simms, 2003, 2007). A
697 direct connection between CAMP volcanism and seismicity seems unlikely considering the distance of the
698 UK from the CAMP itself, and seismic effects of rifting during this time (Tate and Dobson, 1989, Stoker et
699 al., 2017) are more likely. However, it should be noted that the predominant shallow-water heterolithic
700 sandstone/siltstone facies seen in the Cotham Member seismites at Larne and elsewhere (Simms, 2007;
701 Lindström et al., 2015) are particularly prone to soft-sediment deformation (e.g. Couëffé et al., 2004; Owen
702 and Moretti, 2011), whether caused by seismic triggers or not (Owen et al., 2011). Hence it may be that the
703 distribution of supposed seismites in the Rhaetian of NW Europe is a function more of facies distribution
704 during this interval rather than the temporal distribution of seismicity per se. However, the very narrow
705 stratigraphic distribution, with comparable deformation largely absent from similar facies above and below,
706 remains somewhat enigmatic.

707

708 *6.5 Controls on sedimentation*

709 The broad pattern of sedimentation and resulting lithostratigraphy in the Larne Basin (see Section 5; Fig. 11)
710 is consistent with that seen in south-west Britain and has similarities with lithostratigraphic units in the
711 Central European Basin (see Gravendyck et al. 2020). This is interpreted primarily as a response to changes
712 in eustatic sea-level as many of the sedimentological changes can be traced into the Central European Basin
713 (Hesselbo et al., 2004; Barth et al., 2018). Sea-level change during this time included a second-order eustatic
714 rise from Late Triassic into Early Jurassic (Early Sinemurian) that transgressed from west to east, with third-
715 order offlap/onlap cycles superimposed upon this (Barth et al., 2018). The earliest evidence of Late Triassic
716 marine incursion into south-east County Antrim occurs in the grey/green mudstones of the Collin Glen
717 Formation (Boomer et al. 2020) at the top of the Mercia Mudstone Group, probably a lithostratigraphic
718 equivalent of the Blue Anchor Formation of south-west Britain and linked to the Rh1 third-order sequence
719 identified in the Central European Basin (Barth et al., 2018). The base of the overlying Westbury Formation
720 is generally considered erosive across Northern Ireland (Mitchell, 2004) and in south-west Britain (Howard
721 et al., 2008, Gallois 2009, Wilson et al., 1990). Differential uplift and erosion, prior to deposition of the
722 Westbury Formation, may have removed the Collin Glen Formation entirely at the section near Whitehead,
723 which lies toward the basin margin, but the formation appears more complete in the basin centre in the Larne
724 area.

725 The marine sediments of the Westbury Formation reflect a renewed extension of marine environments to
726 form a storm-dominated, shallow epeiric sea (Warrington and Ivimey-Cook, 1995). Movement of faults may
727 have led to differences in the distribution of facies and the thickness, as witnessed at Cloghfin Port (Fig. 7).
728 Overall, the formation across the basin records a change to laminated very dark grey shales and sandstones
729 with marine fossils. The Westbury Formation was interpreted to represent the upper part of the transgressive
730 systems tract by Hesselbo et al. (2004). The formation may equate to much of the second Rhaetian 3rd Order
731 sequence (Rh2) sequence identified by Barth et al. (2018) in the North German Basin, although there is no

732 clear evidence of a sequence boundary within the upper Westbury Formation in the Larne Basin nor, indeed,
733 across the rest of the UK.

734 An abrupt change to shoreface and tidal flat deposits in the lower Cotham Member may reflect local tectonic
735 control of relative sea-level, with the ‘mud-cracked’ surface at the top of the lower Cotham Member in the
736 Larne Basin representing a sequence boundary and lowstand surface. At St Audrie’s Bay this same sequence
737 boundary (Hesselbo et al., 2004) was ascribed to a c.2 m tectonically driven fall in relative sea-level (Mayall,
738 1983) but in the correlative strata of the Larne Basin any effects of sea-level fall, such as facies shifts and
739 erosion, appear more subdued. In sequence stratigraphic terms, the lower Cotham Member was viewed as a
740 lowstand systems tract or falling stage systems tract (Hesselbo et al., 2004), with the overall fining-up trend
741 in the upper Cotham Member (above the ‘mud-cracked’ surface) interpreted as the start of the transgressive
742 systems tract formed by the Hettangian transgression (Hesselbo et al., 2004; Barth et al., 2018), reaching its
743 highstand low in the Waterloo Mudstone Formation at around the *plicatulum* Biohorizon of the Planorbis
744 Zone (Simms and Jeram, 2007).

745 *6.6 Biotic change*

746 Various studies (e.g. Barras and Twitchett, 2007; Mander et al., 2008; Wignall and Bond, 2008; Atkinson et
747 al., 2019; Opazo and Page, 2021) suggest an increase in standing marine biodiversity in the UK through the
748 Westbury Formation into the base of the Cotham Member, followed by a sharp decline to a minimum in the
749 upper Cotham Member and Langport Member and then a gradual recovery into the Planorbis Zone. Wignall
750 and Atkinson (2020) identified two periods of extinction (top Westbury Formation/base Cotham Member
751 and the top of the Langport Member. The lower event was presumed by them to lie within the brackish water
752 deposited upper Cotham Member, but to be ‘hidden’ by these changes in environment (Wignall and
753 Atkinson, 2020). These data are consistent with modest extinction, predominantly of bivalves, through the
754 lower Cotham Member to lower Langport Member interval, as seen in the Waterloo Bay succession (Opazo
755 and Page, 2021). It suggests that these diversity changes began just before the ‘initial’ CIE and reached a
756 peak by the end of the excursion, with recovery underway even as CAMP volcanism continued (Wignall and
757 Bond, 2008). Facies changes linked to sea level through the TJB interval probably influenced benthic faunas
758 (Cope in Radley et al., 2008; Lucas and Tanner, 2008), although they may have had little effect on the
759 difference between faunas of the Westbury Formation and those of the Langport Member and basal Blue
760 Lias Formation because the depositional environments were similar (Twitchett and Mander, in Radley et al.,
761 2008; Mander and Twitchett, 2008). However, if last occurrences of marine invertebrate taxa in the Lilstock
762 Formation were facies controlled then the precise timing and cause of their extinction must remain uncertain.

7. Conclusions and summary

763 The Rhaetian to Hettangian succession in south-east County Antrim shows continuous sedimentation
764 through a time interval encompassing the End Triassic Extinction, the known eruptive phase of the Central

765 Atlantic Magmatic Province and the Triassic–Jurassic Boundary. The key stratigraphic levels recording
766 events associated with the ETE and CAMP are concentrated in and around the Lilstock Formation which
767 preserves a more complete and detailed history of events in the Larne Basin than in south-west Britain. The
768 high-resolution $\delta^{13}\text{C}_{\text{org}}$ profile obtained from the Waterloo Bay section can be correlated with profiles from
769 other regions and allows the events occurring in the Larne Basin and south-west Britain to be placed in the
770 broader context of Pangaea and to tentatively reach the following conclusions:

771 (1) Whilst the Westbury Formation and Cotham Member appear to be affected by regional or
772 eustatic fluctuations in sea-level, the return to normal marine conditions during deposition of the Langport
773 Member may be either a more completely preserved or an expanded section across a gradational transition.
774 This appears to be supported by a more expanded ‘initial’ CIE that extends into the lower Langport Member
775 in the Waterloo Bay carbon isotope curve.

776 (2) As suggested by other authors, the lithostratigraphic base of the Lias Group, as defined by an
777 abrupt increase in TOC preservation, may be diachronous across the UK and therefore reflects differences in
778 water depth and sediment accumulation rate. The upper part of the Langport Member in south-east County
779 Antrim may thus represent a shallow water equivalent of the basal beds of the Blue Lias Formation in the
780 Bristol Channel Basin.

781 (2) In the Larne Basin ammonites appear 5.6 m above the base of the Waterloo Mudstone Formation
782 at Waterloo Bay. The full faunal succession found in south-west Britain, up to the top of the Planorbis Zone,
783 is also present at outcrop in south-east County Antrim, but there is a greater stratigraphic thickness to the
784 biohorizons, particularly in the Planorbis Subzone than in south-west Britain.

785 (3) The $\delta^{13}\text{C}_{\text{org}}$ data obtained from the Waterloo Bay section show an overall pattern through the
786 ‘initial’ CIE similar to the data previously recovered from the nearby Carnduff-2 core and the Bristol
787 Channel Basin, but it is at a significantly higher resolution as a result of finer sample spacing and a
788 stratigraphically expanded succession (compared with the Bristol Channel Basin). Differences in the
789 amplitude of minor (second order) peaks and troughs, probably influenced by local factors, suggest that
790 caution is required if applied to high resolution correlation over longer distances.

791 (4) Based on correlations of the carbon isotope curve proposed here, the Triassic–Jurassic boundary
792 lies between the top of the ‘initial’ CIE (upper part of Bed 13 at Waterloo Bay) and the first ammonites in
793 Bed 24. It therefore rests either within the upper Langport Member (Level 2 on Figure 12) or within the ‘Pre-
794 Planorbis Beds’ of the Waterloo Mudstone Formation (Level 1).

795 (6) The Larne Basin was tectonically active during the TJB interval, as evidenced by synsedimentary
796 fault movements and the occurrence of soft sediment deformed strata that are considered to be seismically
797 disturbed. At Cloghfin Port and Cloghan Point, which are located above the geophysical trace of the
798 Southern Uplands fault zone, there is evidence that tectonic activity exacerbated or influenced a fall in
799 relative sea-level at the transition from the Westbury Formation to the Lilstock Formation. This was
800 followed by further seismicity affecting the lower Cotham Member, representing a protracted series of

801 seismic events. Seismites of similar age are widely distributed in NW Europe and suggest that those in the
802 Larne Basin reflect region-wide tectonism during this time period. This interval is tentatively correlated with
803 a phase of intrusive activity that immediately preceded flood basalt volcanism in the CAMP, potentially
804 indicating an indirect connection between extensional tectonics of the CAMP and the tectonics of the proto-
805 North Atlantic margin.

806 (7) Although tectonics affected sedimentation in the Larne Basin, the major lithological changes are
807 interpreted to relate to regional, presumably eustatic, sea-level change. Facies trends in the Larne Basin
808 broadly resemble those in south-west Britain basins and further into the Central European Basin (Hesselbo et
809 al. 2004; Barth et al., 2018; Gravendyck et al., 2020). There is some evidence for Rhaetian marine influence
810 in the Collin Glen Formation (Boomer et al. 2020), above which the Westbury Formation records a late
811 Rhaetian transgressive-regressive cycle culminating in the lower Cotham Member of the Lilstock Formation.
812 However, evidence suggests that there was subdued erosion at the ‘mud cracked’ surface, marking the top of
813 this sequence at Waterloo Bay. The upper Cotham Member marks the start of a second transgressive
814 sequence that culminated at the Hn7-*plicatulum* Biohorizon in the Planorbis Zone (based on TOC content).

815 (8) The rapid and sustained transgression recorded in the base of the Waterloo Mudstone Formation
816 corresponds with the ‘main’ CIE and peak levels of $p\text{CO}_2$. There is also a loose correspondence between the
817 $p\text{CO}_2$, $\delta^{13}\text{C}$ and sea level records through the T–J boundary in the Larne Basin. Major biotic turnover in the
818 Larne Basin had already occurred before $p\text{CO}_2$ rose significantly above late Rhaetian background levels so
819 this turnover is unlikely to be due to CO_2 -induced climate warming. Although the timing of diversity loss
820 and/or turnover can be constrained only to an interval between the top of the Westbury Formation and the
821 early part of the ‘initial’ CIE in the upper Cotham Member, that interval lies within strata that were deposited
822 under fluctuating salinities.

Acknowledgements

We thank Kamini Manick for performing many of the Waterloo Bay sample geochemical analyses and Paul Wignall and John Walsh for helpful discussions in the field. The Department of the Environment for Northern Ireland are thanked for permission to conduct geochemical sampling at the Waterloo Bay ASSI. This research did not receive any specific grant from funding agencies in the public, commercial, or not-for-profit sectors.

References

823 Anderson, T.B., Parnell, J., Ruffell, A.H., 1995. Influence of basement on the geometry of Permo-Triassic
824 basins in the northwest British Isles. In: Boldy, S.A.R. (Ed.). Permian and Triassic rifting in Northwest
825 Europe. Geological Society Special Publication 10, pp. 103–122.

- 826 Atkinson, J.W., Wignall, P.B., Morton, J.D., Aze, T., 2019. Body size changes in bivalves of the Family
827 Limidae in the aftermath of the end-Triassic mass extinction: The Brobdingnag Effect. *Palaeontology* 62,
828 561–582. Doi:/doi/10.1111/pala.12415.
- 829 Barras, C.G., Twitchett, R.J., 2007. Response of the marine ichnofauna to Triassic-Jurassic environmental
830 change: Ichnological data from southern England. *Palaeogeography, Palaeoclimatology, Palaeoecology* 244,
831 223–241. Doi: [10.1016/j.palaeo.2006.06.040](https://doi.org/10.1016/j.palaeo.2006.06.040).
- 832 Barth, G., Franz, M., Heunisch, C., Ernst, W., Zimmermann, J., Wolfgramm, M., 2018. Marine and
833 terrestrial sedimentation across the T–J transition in the North German Basin. *Palaeogeography,*
834 *Palaeoclimatology, Palaeoecology* 489, 74–94. Doi: [10.1016/j.palaeo.2017.09.029](https://doi.org/10.1016/j.palaeo.2017.09.029).
- 835 Bartolini, A., Guex, J., Spangenberg, J., Schoene, B., Taylor, D., Schaltegger, U., Atudorei, V., 2012.
836 Disentangling the Hettangian carbon isotope record: Implications for the aftermath of the end-Triassic mass
837 extinction. *Geochemistry, Geophysics, Geosystems* 13, Q01007. Doi:10.1029/2011GC003807.
- 838 Benton, M.J., Cook, E., Turner, P., 2002. Permian and Triassic Red Beds and the Penarth Group of Great
839 Britain: Geological Conservation Review Series 24, Joint Nature Conservation Committee, Peterborough,
840 337 pp.
- 841 Blackburn, T.J., Olsen, P.E., Bowring, S.A., McLean, N.M., Kent, D.V., Puffer, J., McHone, G., Rasbury,
842 T.E., Et-Touhami, M., 2013. Zircon U–Pb geochronology links the end-Triassic extinction with the central
843 Atlantic Magmatic Province. *Science* 340, 942–945. Doi:10.1126/science.1234204.
- 844 Bloos, G., Page, K.N., 2000. The basal Jurassic ammonite succession in the North-West European Province
845 – Review and new results. *GeoResearch Forum* 6, 27–40.
- 846 Bond, D.P.G., Wignall, P.B., 2014. Large igneous provinces and mass extinctions: An update. In: Keller, G.,
847 Kerr, A.C., (Eds.), *Volcanism, Impacts, and Mass Extinctions: Causes and Effects*. Geological Society of
848 America Special Paper 505, 29–55. Doi:10.1130/2014.2505(02).
- 849 Bonis, N.R., Ruhl, M., Kürschner, W.M, 2010. Milankovitch-scale palynological turnover across the
850 Triassic-Jurassic transition at St. Audrie’s Bay, SW UK. *Journal of the Geological Society* 167, 877–888.
851 [doi:10.1144/0016-76492009-141](https://doi.org/10.1144/0016-76492009-141).
- 852 Boomer, I., Copestake, P., Raine, R., Azmi, A., Fenton, J., Page, K., O’Callaghan, M., 2020a.
853 Palaeoenvironments and Geochemistry of the Late Triassic to Early Jurassic Interval of County Antrim,
854 Northern Ireland. *Proceedings of the Geologists’ Association*.

- 855 Clémence, M.-E., Hart, M. B. 2013. Proliferation of Oberhauserellidae during the recovery
856 following the Late Triassic extinction: paleoecological implications. *Journal of Paleontology* 87,
857 1004–1015.
- 858 Clémence, M.-E., Bartolini, A., Gardin, S., Paris, G., Beaumont, V., Page, K.N., 2010. Early Hettangian
859 benthic-planktonic coupling at Doniford (SW England): Palaeoenvironmental implications for the aftermath
860 of the end-Triassic crisis. *Palaeogeography, Palaeoclimatology, Palaeoecology* 295, 102–115.
861 Doi:10.1016/j.palaeo.2010.05.021.
- 862 Couëffé, R., Tessier, B., Gigot, P., Beaudoin, B., 2004. Tidal Rhythmites as Possible Indicators of Very
863 Rapid Subsidence in a Foreland Basin: An Example from the Miocene Marine Molasse Formation of the
864 Digne Foreland Basin, SE France. *Journal of Sedimentary Research* 74, 746–759.
865 Doi: 10.1306/040904740746.
- 866 Dal Corso, J., Marzoli, A., Tateo, F., Jenkyns, H.C., Bertrand, H., Youbi, N., Mahmoudi, A., Font, E.,
867 Buratti, N., Cirilli, S., 2014. The dawn of CAMP volcanism and its bearing on the end-Triassic carbon cycle
868 disruption. *Journal of the Geological Society* 171, 153–164. Doi:10.1144/jgs2013-063.
- 869 Donovan, D., Curtis, M., Curtis, S., 1989. A psiloceratid ammonite from the supposed Triassic Penarth
870 Group of Avon, England. *Palaeontology* 32, 231–235.
- 871 Fox, C.P., Cui, X., Whiteside, J.H., Olsen, P.E., Summon, R.E., Grice, K., 2020. Molecular and isotopic
872 evidence reveals the end-Triassic carbon isotope excursion is not from massive exogenous light carbon.
873 *PNAS*, 117, 30171–30178.
- 874 Gallois, R.W., 2007. The stratigraphy of the Penarth Group (late Triassic) of the East Devon coast.
875 *Geoscience in south-west England* 11, 287–297.
- 876 Gallois, R.W., 2009. The Lithostratigraphy of the Penarth Group (late Triassic) of the Severn Estuary area.
877 *Geoscience in south-west England* 12, 71–84.
- 878 Goehring, L., 2013. Evolving fracture patterns: columnar joints, mud cracks and polygonal terrain.
879 *Philosophical Transactions of the Royal Society A: Mathematical, Physical and Engineering Sciences* 371,
880 20120353. Doi:10.1098/rsta.2012.0353.
- 881 Gravendyck et al., 2020
- 882 Griffith, A.E., Wilson, H.E., 1982. Geology of the country around Carrickfergus and Bangor. *Geological*
883 *Survey of Northern Ireland Memoir, Sheet 29*. 118 pp.

- 884 Guex, J., Bartolini, A., Atudorei, V., Taylor, D., 2004. High resolution ammonite and carbon isotope
885 stratigraphy across the Triassic-Jurassic boundary at New York Canyon (Nevada). *Earth and Planetary*
886 *Science Letters* 225, 29–41. Doi:10.1016/j.epsl.2004.06.006.
- 887 Guex, J., Schoene, B., Bartolini, A., Spangenberg, J., Schaltegger, U., O’Dogherty, L., Taylor, D., Bucher,
888 H., Atudorei, V., 2012. Geochronological constraints on post-extinction recovery of the ammonoids and
889 carbon cycle perturbations during the Early Jurassic. *Palaeogeography, Palaeoclimatology, Palaeoecology*
890 346–347, 1–11. Doi:10.1016/j.palaeo.2012.04.030.
- 891 Hallam, A., 1960. The White Lias of the Devon Coast. *Proceedings of the Geologists’ Association* 71, 47-60.
- 892 Hallam, A., Wignall, P.B., 1999. Mass Extinctions and Sea-level Changes. *Earth-Science Reviews* 8, 217–
893 250.
- 894 Hamilton, D. 1961. Algal growths in the Rhaetic Cotham Marble of southern England. *Palaeontology* 4,
895 324–333.
- 896 Heimdal, T.H., Callegaro, S., Svensen, H.H., Jones, M.T., Pereira, E., Planke, S., 2019. Evidence for
897 magma–evaporite interactions during the emplacement of the Central Atlantic Magmatic Province (CAMP)
898 in Brazil. *Earth and Planetary Science Letters* 506, 476-492. doi:10.1038/s41598-017-18629-8.
- 899 Heimdal, T.H., Svensen, H. H., Ramezani, J., Iyer, K., Pereira, E., Rodrigues, R., Jones, M.T., Callegaro, S.,
900 2018. Large-scale sill emplacement in Brazil as a trigger for the end-Triassic crisis. *Scientific Reports*, 8, 141
901 (2018). Doi:10.1038/s41598-017-18629-8.
- 902 Hesselbo, S.P., Robinson, S.A., Surlyk, F., Piasecki, S., 2002. Terrestrial and marine mass extinction at the
903 Triassic–Jurassic boundary synchronized with major carbon-cycle perturbation: A link to initiation of
904 massive volcanism? *Geology* 30, 251–254. Doi:10.1130/0091-7613(2002)030<0251:TAMEAT>2.0.CO;2.
- 905 Hesselbo, S.P., Robinson, S.A. and Surlyk, F., 2004. Sea-level change and facies development across
906 potential Triassic–Jurassic boundary horizons, SW Britain. *Journal of the Geological Society, London* 161,
907 365–379. Doi:10.1144/0016-764903-033.
- 908 Hillebrandt, A.v., 1994. The Triassic/Jurassic boundary and Hettangian biostratigraphy in the area of the
909 Utcubamba Valley (northern Peru). *Geobios* 27, supplement 2, 297–307. doi: 10.1016/S0016-
910 6995(94)80148-7.

- 911 Hillebrandt, A. v., Krystyn, L., 2009. On the oldest Jurassic ammonites of Europe (Northern Calcareous
912 Alps, Austria) and their global significance. *Neues Jahrbuch für Geologie und Paläontologie –*
913 *Abhandlungen* 253, 163–195. Doi: 10.1127/0077-7749/2009/0253-0163.
- 914 Hillebrandt, A.v., Krystyn, L., Kürschner, W.M., 2007. A candidate GSSP for the base of the Jurassic in the
915 Northern Calcareous Alps (Kujoch section, Karwendel Mountains, Tyrol, Austria). *International*
916 *Subcommission on Jurassic Stratigraphy Newsletter* 34, 2–20.
- 917 Hillebrandt, A.v., Krystyn, L., Kürschner, W.M., Bonis, N.R., Ruhl, M., Richoz, S., Urlichs, M., Bown, P.R.,
918 Kment, K., McRoberts, C.A., Simms, M.J., Tomášovych, A., 2013. The Global Stratotype Sections and
919 Point (GSSP) for the base of the Jurassic System at Kuhjoch (Karwendel Mountains, Northern Calcareous
920 Alps, Tyrol, Austria). *Episodes* 36, 162–198.
- 921 Hodges, P. 2021. A new ammonite from the Penarth Group, South Wales and the base of the Jurassic System
922 in south-west Britain. *Geological Magazine* 158, 1109–1114.
- 923 Hüsing, S.K., Beniést, A., van der Boon, A., Abels, H.A., Deenen, M.H.L., Ruhl, M., Krijgsman, W., 2014.
924 Astronomically-calibrated magnetostratigraphy of the Lower Jurassic marine successions at St. Audrie's Bay
925 and East Quantoxhead (Hettangian–Sinemurian; Somerset, UK). *Palaeogeography, Palaeoclimatology,*
926 *Palaeoecology* 403, 43–56. Doi:10.1016/j.palaeo.2014.03.022.
- 927 Ivimey-Cook, H.C., 1975. The stratigraphy of the Rhaetic and Lower Jurassic in East Antrim. *Bulletin of the*
928 *Geological Survey of Great Britain* 50, 51–69.
- 929 Jaraula, C.M.B., Grice, K., Twitchett, R.J., Böttcher, M.E., LeMetayer, P., Dastidar, A.G., Opazo, L-F.,
930 2013. Elevated pCO₂ leading to Late Triassic extinction, persistent photic zone euxinia, and rising sea levels.
931 *Geology* 41, 955–958. Doi:10.1130/g34183.1.
- 932 Kent, D.V., Olsen, P.E., Muttoni, G., 2017. Astrochronostratigraphic polarity time scale (APTS) for the Late
933 Triassic and Early Jurassic from continental sediments and correlation with standard marine stages. *Earth*
934 *Science Reviews* 166, 153–180. Doi:10.1016/j.earscirev.2016.12.014.
- 935 Korte, C., Hesselbo, S.P., Jenkyns, H.C., Rickaby, R.E.M., Spötl, C., 2009. Palaeoenvironmental
936 significance of carbon- and oxygen-isotope stratigraphy of marine Triassic–Jurassic boundary sections in
937 SW Britain. *Journal of the Geological Society, London* 166, 431–445. Doi:10.1144/0016-76492007-177.
- 938 Korte, C., Kozur, H.W., 2011. Bio- and chemostratigraphic assessment of carbon isotope records across the
939 Triassic–Jurassic boundary at Csóvár quarry (Hungary) and Kendlbachgraben (Austria) and implications for
940 global correlations. *Bulletin of the Geological Society of Denmark* 59, 101–115.

- 941 Korte, C., Ruhl, M., Pálffy, J., Ullmann, C.V., Hesselbo, S.P., 2019. Chemostratigraphy across the Triassic–
942 Jurassic Boundary. In: Sial, A.N., Gaucher, C., Ramkumar, M., Ferreira, V.P. (Eds.), Chemostratigraphy
943 Across Major Chronological Boundaries. Geophysical Monograph 2, 185–210.
944 Doi:[10.1002/9781119382508.ch10](https://doi.org/10.1002/9781119382508.ch10).
- 945 Kürschner, W.M., Bonis, N.R., Krystyn, L., 2007. Carbon-isotope stratigraphy and palynostratigraphy of the
946 Triassic–Jurassic transition in the Tiefengraben section: Northern Calcareous Alps (Austria).
947 Palaeogeography, Palaeoclimatology, Palaeoecology 244, 257–280. Doi:[10.1016/j.palaeo.2006.06.031](https://doi.org/10.1016/j.palaeo.2006.06.031).
- 948 Laborde-Casadaban, M., Homberg, C., Schnyder, J., Borderie, S., Raine, R., 2021. Do soft sediment
949 deformations in the Late Triassic and Early Jurassic of the UK record seismic activity during the break-up of
950 Pangea? Proceedings of the Geologists' Association (This Volume).
- 951 Lindström, S., van de Schootbrugge, B., Dybkjaer, K., Pedersen, G.K., Fiebig, J., Nielsen, L.H., Richoz, S.,
952 2012. No causal link between terrestrial ecosystem change and methane release during the end-Triassic mass
953 extinction. *Geology* 40, 531–534. Doi:[10.1130/g32928.1](https://doi.org/10.1130/g32928.1).
- 954 Lindström, S., Pedersen, G.K., van de Schootbrugge, B., Hansen, K.H., Kuhlmann, N., Thein, J., Johansson,
955 L., Petersen, H.I., Alwmark, C., Dybkjær, K., Weibel, R., Erlström, M., Nielsen, L.H., Oschmann, W.,
956 Tegner, C., 2015. Intense and widespread seismicity during the end-Triassic mass extinction due to
957 emplacement of a large igneous province. *Geology* 43, 387–390. Doi: <https://doi.org/10.1130/G36444.1>
- 958 Lindström, S., van de Schootbrugge, B., Hansen, K.H., Pedersen, G.K., Alsen, P., Thibault, N., Dybkjær, K.,
959 Bjerrum, C.J., Nielsen, L.H., 2017. A new correlation of Triassic–Jurassic boundary successions in NW
960 Europe, Nevada and Peru, and the Central Atlantic Magmatic Province: A time-line for the end-Triassic
961 mass extinction. *Palaeogeography, Palaeoclimatology, Palaeoecology* 478, 80–102. Doi:
962 [10.1016/j.palaeo.2016.12.025](https://doi.org/10.1016/j.palaeo.2016.12.025).
- 963 Lindström, S., Sanei, H., van de Schootbrugge, B., Pedersen, G.K., Leshner, C.E., Tegner, C., Heunisch, C.,
964 Dybkjær, K., Outridge, P.M., 2019. Volcanic mercury and mutagenesis in land plants during the end-Triassic
965 mass extinction. *Science Advances* 5, eaaw4018. Doi: [10.1126/sciadv.aaw4018](https://doi.org/10.1126/sciadv.aaw4018).
- 966 Lucas, S., Tanner, L., 2008. Reexamination of the end-Triassic Mass Extinction. In: Elewa, A.F.T. (Ed.),
967 Mass Extinction. Springer-Verlag, Berlin, Heidelberg, pp. 66–103. Doi: [10.1007/978-3-540-75916-4](https://doi.org/10.1007/978-3-540-75916-4).
- 968 Lucas, S.G., Tanner, L.H., 2015. End-Triassic nonmarine biotic events. *Journal of Palaeogeography* 4, 331–
969 348. Doi:[10.1016/j.jop.2015.08.010](https://doi.org/10.1016/j.jop.2015.08.010).

- 970 Macquaker, J.H.S., 1999. 4. Aspects of the Sedimentology of the Westbury Formation. In: Swift, A. and
971 Martill, D.M. (Eds.), Fossils of the Rhaetian Penarth Group. The Palaeontological Association, London, pp.
972 39–48.
- 973 Mander, L., Twitchett, R.J., 2008. Quality of the Triassic–Jurassic bivalve fossil record in northwest Europe.
974 *Palaeontology* 51, 1213–1223. Doi:10.1111/j.1475-4983.2008.00821.x.
- 975 Mander, L., Twitchett, R.J., Benton, M.J., 2008. Palaeoecology of the late Triassic extinction event in the
976 SW UK. *Journal of the Geological Society, London* 165, 319–332.
- 977 Manning, P.I., Robbie, J.A., Wilson, H.E., Hawkes, J.R., Hughes, M.J., McAllister, J.S.V., Pattison, J.,
978 Warrington, J., 1970. Geology of Belfast and the Lagan Valley. *Memoirs of the Geological Survey of*
979 *Northern Ireland*, sheet 36.
- 980 Manning, P.I., Wilson, H.E., 1975. I. The stratigraphy of the Larne Borehole, County Antrim. *Bulletin of the*
981 *Geological Survey of Great Britain* 50, 1–50.
- 982 Mayall, M.J., 1981. The Late Triassic Blue Anchor Formation and the initial Rhaetian marine transgression
983 in south-west Britain. *Geological Magazine* 118, 377–384.
- 984 Mayall, M.J., 1983. An earthquake origin for synsedimentary deformation in a late Triassic (Rhaetian)
985 lagoonal sequence, southwest Britain. *Geological Magazine* 120, 613–622.
- 986 McElwain, J.C., Beerling, D.J., Woodward, F.I., 1999. Fossil plants and global warming at the Triassic–
987 Jurassic Boundary. *Science* 285, 1386–1390. Doi:10.1126/science.285.5432.1386.
- 988 McElwain, J.C., Wagner, P.J., Hesselbo, S.P., 2009. Fossil plant relative abundances indicate sudden loss of
989 Late Triassic biodiversity in east Greenland. *Science* 324, 1554–1556. Doi:10.1126/science.1171706.
- 990 McHone, J.G., 2003, Volatile emissions from Central Atlantic magmatic province basalts: Mass assumptions
991 and environmental consequences. In: Hames, W.E., McHone, J.G., Renne, P.R., Ruppel, C., (Eds.), *The*
992 *Central Atlantic Magmatic Province: Insights from Fragments of Pangea*. American Geophysical Union
993 *Geophysical Monograph* 136, pp. 241–254.
- 994 McMahon, S., van Smeerdijk Hood, A., McIlroy, D., 2016. The origin and occurrence of subaqueous
995 sedimentary cracks. *Geological Society, London, Special Publications* 448, 285–309. Doi:10.1144/SP448.15.
- 996 Mitchell, W.I. (Ed.), 2004. *The Geology of Northern Ireland – Our Natural Foundation*. Geological Survey
997 of Northern Ireland, Belfast, pp. 318.
- 998 Moretti, M., van Loon, A.J. (Tom), 2014. Restrictions to the application of ‘diagnostic’ criteria for
999 recognizing ancient seismites. *Journal of Palaeogeography*, 3, 162–173. Doi: 10.3724/SP.J.1261.2014.00050.

- 1000 Onoue, T., Sato, H., Yamashita, D., Ikehara, M., Yasukawa, K., Fujinaga, K., Kato, Y., Matsuoka, A., 2016.
1001 Bolide impact triggered the Late Triassic extinction event in equatorial Panthalassa. *Scientific Reports*
1002 6, 29609 (2016). Doi:10.1038/srep29609.
- 1003 Opazo, L-F., Page, K.N., 2021. Palaeoecological patterns of change in marine invertebrate faunas across the
1004 end-Triassic mass extinction event: evidence from Larne, Northern Ireland. *Proceedings of the Geologists’*
1005 *Association* (This Volume).
- 1006 Owen, G., Moretti, M., 2011. Identifying triggers for liquefaction-induced soft-sediment deformation in
1007 sands. *Sedimentary Geology* 235, 141–147. Doi:10.1016/j.sedgeo.2010.10.003.
- 1008 Owen, G., Moretti, M., Alfaro, P., 2011. Recognising triggers for soft-sediment deformation: Current
1009 understanding and future directions. *Sedimentary Geology* 235, 133–140.
1010 Doi:10.1016/j.sedgeo.2010.12.010.
- 1011 Page, K.N. 2010. Ammonites. In: Lord, A.R., Davis, P.G., (Eds.), *Fossils from the Lower Lias of the Dorset*
1012 *Coast, Palaeontological Association Field Guide to Fossils* 13, pp 169-261.
- 1013 Pálffy, J., Demény, A., Haas, J., Carter, E.S., Görög, Á., Halász, D., Oravecz-Scheffer, A., Hetényi, M.,
1014 Márton, E., Orchard, M.J., Ozsvárt, P., Vető, I., Zajzon, N., 2007. Triassic-Jurassic boundary events inferred
1015 from integrated stratigraphy of the Csővár section, Hungary. *Palaeogeography, Palaeoclimatology,*
1016 *Palaeoecology* 244, 11–33. Doi:10.1016/j.palaeo.2006.06.021.
- 1017 Pálffy, J., Kocsis, Á.T., 2014. Volcanism of the Central Atlantic magmatic province as the trigger of
1018 environmental and biotic changes around the Triassic-Jurassic boundary. In: Keller, G., Kerr, A.C., (Eds.),
1019 *Volcanism, Impacts, and Mass Extinctions: Causes and Effects. Geological Society of America Special*
1020 *Paper* 505, 245–261. Doi:10.1130/2014.2505(12).
- 1021 Percival, L.M.E., Ruhl, M., Hesselbo, S.P., Jenkyns, H.C., Mather, T.A., Whiteside, J.H., 2017. Mercury
1022 evidence for pulsed volcanism during the end-Triassic mass extinction. *Proceedings of the National*
1023 *Academy of Sciences of the United States of America* 114, 7929–7934. Doi:10.1073/pnas.1705378114.
- 1024 Poole, E.G., Whiteman, A.J., 1966. *Geology of the country around Nantwich and Whitchurch. British*
1025 *Geological Survey Memoir, One-inch Sheet* 122.
- 1026 Portlock, J.E., 1843. *Report on the geology of the county of Londonderry and parts of Tyrone and*
1027 *Fermanagh. Andrew Milliken, Dublin and London,* 784 pp.
- 1028 Pratt, B., 1998. Syneresis cracks: Subaqueous shrinkage in argillaceous sediments caused by earthquake-
1029 induced dewatering. *Sedimentary Geology* 117, 1–10. Doi: 10.1016/S0037-0738(98)00023-2.

- 1030 Radley, J.D., Twitchett, R.J., Mander, L., Cope, J.C.W., 2008. Discussion on palaeoecology of the Late
1031 Triassic extinction event in the SW UK. *Journal of the Geological Society* 165, 988–992.
1032 Doi:10.1144/001676492008-014.
- 1033 Raine, R., Copestake, P., Simms, M.J., Boomer, I., 2020. Uppermost Triassic to Lower Jurassic sediments of
1034 the island of Ireland and its surrounding basins. *Proceedings of the Geologists' Association (This Volume)*.
- 1035 Raine, R., Fenton, J.P.G., Boomer, I., Azmi, A., Copestake, P., 2021. Uppermost Triassic to Lower
1036 Jurassic stratigraphy in the Lough Foyle Basin of County Londonderry, Northern Ireland.
1037 *Proceedings of the Geologists' Association (This Volume)*.
- 1038 Reynaud, J.-Y., Dalrymple, R. W., 2012. Shallow-marine tidal deposits. In: Davis Jr., R.A., Dalrymple, R.W.
1039 (Eds.), *Principles of tidal sedimentology*. Springer, Berlin, Heidelberg, pp. 335–369. Doi: 10.1007/978-94-
1040 007-0123-6_13.
- 1041 Reid, C.G.R., Bancroft, A.J., 1986. The Irish Lower Jurassic type ammonites of Major-General J.E. Portlock
1042 (1843): *Leptechioceras macdonnelli*, *Psiloceras (Caloceras) intermedium*, and *Psiloceras (Psiloceras)*
1043 *sampsoni*. *Irish Journal of Earth Sciences* 8, 41–51.
- 1044 Richardson, L., 1911. The Rhaetic and contiguous deposits of West, Mid and part of East Somerset.
1045 *Quarterly Journal of the Geological Society, London* 67, 1–74.
- 1046 Ruhl, M., Hesselbo, S.P., Al-Suwaidi, A., Jenkyns, H.C., Damborenea, S.E., Manceñido, M.O., Storm, M.,
1047 Mather, T.A., Riccardi, A.C., 2020. On the onset of Central Atlantic Magmatic Province (CAMP) volcanism
1048 and environmental and carbon-cycle change at the Triassic–Jurassic transition (Neuquén Basin, Argentina).
1049 *Earth-Science Reviews* 208 (2020) 103229.
- 1050 Ruhl, M., Kürschner, W.M., 2011. Multiple phases of carbon cycle disturbance from large igneous province
1051 formation at the Triassic–Jurassic transition. *Geology* 39, 431–434. Doi:10.1130/g31680.1.
- 1052 Ruhl, M., Kürschner, W.M., Krystyn, L., 2009. Triassic–Jurassic organic carbon isotope stratigraphy of key
1053 sections in the western Tethys realm (Austria). *Earth and Planetary Science Letters* 281, 169–187.
1054 Doi:10.1016/j.epsl.2009.02.020.
- 1055 Schaller, M.F., Wright, J.D., Kent, D.V., 2011. Atmospheric pCO₂ perturbations associated with the Central
1056 Atlantic Magmatic Province. *Science* 331, 1404–1409. Doi:10.1126/science.1199011.
- 1057 Schaller, M.F., Wright, J.D., Kent, D.V., Olsen, P.E., 2012. Rapid emplacement of the Central Atlantic
1058 Magmatic Province as a net sink for CO₂. *Earth and Planetary Science Letters* 323–324, 27–39.
1059 Doi:10.1016/j.epsl.2011.12.028.

- 1060 Schobben, M., van de Schootbrugge, B., Wignall, P.B., 2019. Interpreting the carbon isotope records of mass
1061 extinctions. *Elements* 15, 331–337. Doi: 10.2138/gselements.15.5.331.
- 1062 Siebach, K.L., Grotzinger, J.P., Kah, L.C., Stack, K.M., Malin, M., L veill , R., Sumner, D.Y., 2014.
1063 Subaqueous shrinkage cracks in the Sheepbed mudstone: Implications for early fluid diagenesis, Gale crater,
1064 Mars. *Journal of Geophysical Research, Planets* 119, 1597–1613. Doi:10.1002/2014JE004623.
- 1065 Simms, M.J., 2003. Uniquely extensive seismite from the latest Triassic of the United Kingdom: evidence
1066 for bolide impact? *Geology* 31, 557–560. Doi:10.1130/0091-7613(2003)031<0557:UESFTL>2.0.CO;2.
- 1067 Simms, M.J., 2007. Uniquely extensive soft-sediment deformation in the Rhaetian of the UK: evidence for
1068 earthquake or impact? *Palaeogeography, Palaeoclimatology, Palaeoecology* 244, 407–423.
1069 Doi:10.1016/j.palaeo.2006.06.037.
- 1070 Simms, M.J., 2021. Fossil echinoderms from the Triassic and Jurassic of Ireland. *Proceedings of the*
1071 *Geologists' Association* (This Volume).
- 1072 Simms, M.J., Chidlaw, N., Morton, N., Page, K.N., 2004. British Lower Jurassic Stratigraphy. *Geological*
1073 *Conservation Review Series*, Joint Nature Conservation Committee, pp. 458.
- 1074 Simms, M.J., Edmunds, M. 2021. Ammonites from the Lias Group (Lower Jurassic, Sinemurian and
1075 Pliensbachian) of White Park Bay, Co. Antrim, Northern Ireland. *Proceedings of the Geologists' Association*
1076 (This Volume)
- 1077 Simms, M.J., Jeram, A.J., 2007. Waterloo Bay, Larne, Northern Ireland: a candidate Global Stratotype
1078 Section and Point for the base of the Hettangian Stage and Jurassic System. *International Subcommission on*
1079 *Jurassic Stratigraphy Newsletter* 34, 50–68.
- 1080 Simms, M.J., Smyth, R.S.H., Martill, D.M., Collins, P.C., Byrne, R., 2020. First dinosaur remains from
1081 Ireland. *Proceedings of the Geologists' Association* (This Volume).
- 1082 Smith, A.B., McGowan, A.J., 2007. The shape of the Phanerozoic marine palaeodiversity curve: How much
1083 can be predicted from the sedimentary rock record of Western Europe? *Palaeontology* 50, 765–774.
1084 Doi:10.1111/j.1475-4983.2007.00693.x.
- 1085 Steinhorsdottir, M., Elliott-Kingston, C., Bacon, K.L., 2018. Cuticle surfaces of fossil plants as a potential
1086 proxy for volcanic SO₂ emissions: observations from the Triassic–Jurassic transition of East Greenland.
1087 *Palaeobiodiversity and Palaeoenvironments* 98, 49–69. Doi:10.1007/s12549-017-0297-9.
- 1088 Steinhorsdottir, M., Jeram, A.J., McElwain, J.C., 2011. Extremely elevated CO₂ concentrations at the
1089 Triassic/Jurassic boundary. *Palaeogeography, Palaeoclimatology, Palaeoecology* 308, 418–432.
1090 Doi:10.1016/j.palaeo.2011.05.050.

- 1091 Storm, M.S., Hesselbo, S.P., Jenkyns, H.C., Ruhl, M., Ullmann, C.V., Xu, W., Leng, M.J., Riding, J.B., Olga
1092 Gorbanenko, O., 2020. Orbital pacing and secular evolution of the Early Jurassic carbon cycle. *PNAS*, 117,
1093 3974–3982.
- 1094 Stoker, M.S., Stewart, M.A., Shannon, P.M., Bjerager, M., Nielsen, T., Blischke, A., Hjelstuen, B.O., Gaina,
1095 C., McDermott, K., Ólavsdóttir, J., 2017. An overview of the Upper Palaeozoic–Mesozoic stratigraphy of the
1096 NE Atlantic region. *Geological Society, London, Special Publications* 447, 11–68. Doi:10.1144/SP447.2.
- 1097 Svensen, H., Planke, S., Chevallier, L., Malthe-Sorensen, A., Corfu, F., Jamtveit, B., 2007. Hydrothermal
1098 venting of greenhouse gases triggering Early Jurassic global warming. *Earth and Planetary Science Letters*,
1099 256, 554–566. doi:10.1016/j.epsl.2007.02.013.
- 1100 Swift, A., 1995. A review of the nature and outcrop of the ‘White Lias’ facies of the Langport Member
1101 (Penarth Group: Upper Triassic) in Britain. *Proceedings of the Geologists’ Association* 106, 247–258.
- 1102 Swift, A. 1999. 2. Stratigraphy (including biostratigraphy). In: Swift, A., Martill, D.M. (Eds.), 1999. *Fossils*
1103 *of the Rhaetian Penarth Group. Field Guide to Fossils No. 9, Palaeontological Association, London, pp. 15–*
1104 *30.*
- 1105 Tate, R., 1867. On the Lower Lias of the north-east of Ireland. *Quarterly Journal of the Geological Society*,
1106 *London* 23, 291–305.
- 1107 Tate, M., Dobson, M., 1989. Late Permian to early Mesozoic rifting and sedimentation offshore NW Ireland.
1108 *Marine and Petroleum Geology* 6, 49–59. doi:10.1016/0264-8172(89)90075-5.
- 1109 Thibodeau, A.M., Ritterbush, K., Yager, J.A., West, A.J., Ibarra, Y., Bottjer, D.J., Berelson, W.M.,
1110 Bergquist, B.A., Corsetti, F.A., 2016. Mercury anomalies and the timing of biotic recovery following the
1111 end-Triassic mass extinction. *Nature Communications* 7, 11147 (2016). doi:10.1038/ncomms11147.
- 1112 van de Schootbrugge, B., Bachan, A., Suan, G., Richoz, S., Payne, J.L., 2013. Microbes, mud and methane:
1113 Cause and consequence of recurrent Early Jurassic anoxia following the end-Triassic mass extinction.
1114 *Palaeontology* 56, 685–709. doi:10.1111/pala.12034.
- 1115 Warrington, G., Audley-Charles, M.G., Elliott, R.E., Evans, W.B., Ivimey-Cook, H.C., Kent, P.E., Robinson,
1116 P.L., Shotton, F.W., Taylor, F.M., 1980. A correlation of Triassic rocks in the British Isles. *Geological*
1117 *Society of London Special Report*, 13, Blackwell Scientific, pp. 78.
- 1118 Warrington, G., Cope, J.C.W., Ivimey-Cook, H.C., 1994. St Audrie’s Bay, Somerset, England: A candidate
1119 Global Stratotype Section and Point for the base of the Jurassic System. *Geological Magazine* 131, 191–200.
1120 doi:10.1017/S0016756800010724.

- 1121 Warrington, G., Cope, J.C.W., Ivimey-Cook, H.C., 2008. The St Audries Bay – Doniford Bay section,
1122 Somerset, England: Updated proposal for a candidate Global Stratotype Section and Point for the base of the
1123 Hettangian Stage, and of the Jurassic System. International Subcommission on Jurassic Stratigraphy
1124 Newsletter 35, 2–66.
- 1125 Warrington, G., Harland, R., 1975. Palynology of the Trias and Lower Lias of the Larne Borehole. Bulletin
1126 of the Geological Survey of Great Britain 50, 37-50.
- 1127 Warrington, G., Ivimey-Cook, H.C., 1992. Triassic. In: Cope, J.C.W., Ingham, J.K. and Rawson, P.F. (Eds.),
1128 Atlas of palaeogeography and lithofacies. Memoirs of the Geological Society, London 13, pp. 97–106.
- 1129 Weedon, G., Jenkyns, H., Page, K., 2018. Combined sea-level and climate controls on limestone formation,
1130 hiatuses and ammonite preservation in the Blue Lias Formation, South Britain (uppermost Triassic – Lower
1131 Jurassic). Geological Magazine 155, 1117–1149. doi:10.1017/S001675681600128X.
- 1132 Weedon, G., Page, K., Jenkyns, H., 2019. Cyclostratigraphy, stratigraphic gaps and the duration of the
1133 Hettangian Stage (Jurassic): Insights from the Blue Lias Formation of southern Britain. Geological
1134 Magazine 156, 1469–1509. doi:10.1017/S0016756818000808.
- 1135 Whiteside, J.H., Olsen, P.E., Eglinton, T., Brookfield, M.E., Sambrotto, R.N., 2010. Compound-specific
1136 carbon isotopes from Earth’s largest flood basalt eruptions directly linked to the end-Triassic mass
1137 extinction. Proceedings of the National Academy of Sciences of the USA 107, 6721–6725.
- 1138 Wignall, P.B., Atkinson, J.W., 2020. A two-phase end-Triassic mass extinction. Earth-Science Reviews 208
1139 (2020) 103282.
- 1140
- 1141 Wignall, P.B., Bond, D.P.G., 2008. The end-Triassic and Early Jurassic mass extinction records in the
1142 British Isles. Proceedings of the Geologists' Association 119, 73–84. doi:10.1016/S0016-7878(08)80259-3.
- 1143 Wilson, H.E, Manning, P.I., 1978. Geology of the Causeway Coast. Memoir of the Geological Survey of
1144 Northern Ireland, Sheet 7 (Northern Ireland).
- 1145 Wilson, D., Davies, J.R., Fletcher, C.J.N., Smith, M., 1990. Geology of the South Wales Coalfield, Part VI,
1146 the Country Around Bridgend. Memoir of the British Geological Survey England and Wales Sheets 261 and
1147 262. HMSO, London, pp. 62.
- 1148 Yager, J.A., West, A.J., Corsetti, F.A., Berelson, W.M., Rollins, N.E., Rosas, S., Bottjer, D.J., 2017.
1149 Duration of and decoupling between carbon isotope excursions during the end-Triassic mass extinction and
1150 Central Atlantic Magmatic Province emplacement. Earth and Planetary Science Letters 473, 227–236.
1151 doi:10.1016/j.epsl.2017.05.031.

Figure captions

1152 **Figure 1.** Geology of south-east County Antrim showing localities described or referred to in the paper. Left
 1153 inset shows the locations of Waterloo Bay and the Larne-1 Borehole. Bottom right inset shows location of
 1154 the Rathlin-Foyle (RF) and Larne-Lough Neagh (LLN) basins within Northern Ireland.

1155

1156 **Figure 2.** Sketch map of the Triassic–Jurassic boundary succession exposed on the wave-cut platform at
 1157 Waterloo Bay, Larne (modified after Ivimey-Cook, 1975). Strata dip to the northwest at 20° – 30° .

1158

1159 **Figure 3.** Carbon stable isotopes and TOC plotted against graphic log of the section at Waterloo Bay, Larne.
 1160 Samples span the interval from above the ‘mud cracked’ horizon at the base of the upper Cotham Member to
 1161 the first common occurrence of *P. plicatulum* in the Waterloo Mudstone Formation. **A**, carbon stable-
 1162 isotopes (bulk organic carbon); **B**, carbonate (%); **C**, total organic carbon (%). Sedimentary log after Simms
 1163 and Jeram (2007), with bed numbers referred to in text.

1164

1165 **Figure 4.** Ammonites from the basal Hettangian. All specimens from Waterloo Bay, Larne, Co. Antrim,
 1166 unless stated otherwise. Specimens to same scale, except b, c and k. Scale bar = 5 cm.

1167 **a** *Psiloceras erugatum* (Phillips, 1829). Large uncrushed plicate example from nodule in middle of
 1168 Bed 24. K2014.1.9

1169 **b, c** Detail of sutures on K2014.1.9

1170 **d** *Psiloceras erugatum* (Phillips, 1829). From ex situ nodule, shore below Mullaghdubh House,
 1171 Islandmagee, Co. Antrim. K2014.1.23

1172 **e** *Psiloceras erugatum* (Phillips, 1829). From same nodule as ‘a’

1173 **f** *Psiloceras planorbis* (J. de C. Sowerby, 1824). Crushed example, 20 cm above base of Bed 28a.
 1174 K2014.1.47

1175 **g** *Psiloceras planorbis* (J. de C. Sowerby, 1824). Crushed examples, 4cm above base of Bed 28a.
 1176 These are stratigraphically the earliest examples of this species found at Larne.

1177 **h** *Psiloceras* sp.. Crushed involute specimen, 15 cm above base of Bed 25 or possibly Bed 26. A
 1178 specimen of *Modiolus minimus* and part of an ambulacrum of *Diademopsis*, are visible in the lower part of
 1179 the block. K2014.1.138

1180 **i** *Psiloceras sampsoni* (Portlock, 1843). Partly crushed pyritic example, 6 cm above the base of Bed
 1181 29. K2014.1.49

1182 **j** *Neophyllites cf. antecedens* Lange, 1941. Pyritic example, Ex situ, The Gobbins, Islandmagee, Co.
 1183 Antrim. K2014.1.12

- 1184 **k** Detail of sutures on K2014.1.12
- 1185 **l** *Psiloceras plicatulum* (Quenstedt, 1883). Crushed example, top of Bed 28b. K2014.1.48
- 1186
- 1187 **Figure 5.** Ammonites from the basal Hettangian. All specimens from Waterloo Bay, Larne, Co. Antrim,
 1188 unless stated otherwise. Specimens to same scale, except b, d, f and g. Scale bar = 5 cm.
- 1189 **a** *Neophyllites imitans* Lange, 1941. Uncrushed example from marl in middle of bed 25. K2014.1.16
- 1190 **b, f** Detail of sutures on K2014.1.16
- 1191 **c, d** *Neophyllites antecedens* Lange, 1941. Pyritic internal cast, 6 cm below the top of bed 26.
 1192 K2014.1.14
- 1193 **e** *Neophyllites antecedens* Lange, 1941. 25 cm above base of bed 27. K2014.1.15
- 1194 **g** Drawing of suture, specimen K2014.1.14 (c, d)
- 1195 **h** *Neophyllites* sp. ex grp. *Becki* (Schmidt, 1925). Strongly ribbed specimen from top of bed 26.
 1196 K2014.1.13
- 1197 **i** *Psiloceras plicatulum* (Quenstedt, 1883). Uncrushed pyritic internal cast, *ex situ*, Minnis North, near
 1198 Glenarm, Co. Antrim. K2014.1.7
- 1199 **j** *Caloceras intermedium* (Portlock, 1843). Uncrushed example from limestone, *ex situ*, Minnis North,
 1200 near Glenarm, Co. Antrim. K2014.1.120
- 1201 **k** *Caloceras intermedium* (Portlock, 1843). Partly crushed example, Johnstoni Subzone. K2014.1.52
- 1202 **l** *Caloceras johnstoni* (J. de C. Sowerby, 1824). Uncrushed example, *ex situ* from limestone,
 1203 Johnstoni Subzone. A specimen of *Pinna* cf. *similes* obscures the right-hand side of this specimen.
 1204 K2014.1.1
- 1205 **m** *Psiloceras plicatulum* (Quenstedt, 1883). Crushed example (left) associated with *Caloceras* sp., 20
 1206 cm below top of Bed 33e. K2014.1.50
- 1207
- 1208 **Figure 6.** Cloghan Point, Whitehead.
- 1209 **a,** Lithostratigraphy and composite log of the section.
- 1210 **b,** Sketch map of outcrop, with mapped units coloured according to lithostratigraphy in **a**.
- 1211 **c,** Cliff section, with upper Cotham Member limestone interval starting approximately across centre of
 1212 image, and red-brown lower Cotham Member mudstones 1.5 m below. Dashed red line indicates Fault A
 1213 (see map **b**).
- 1214 **d–f,** Junction between Westbury Formation and Lilstock Formation exposed after beach deposits stripped
 1215 away by storms.

1216 **d**, Exposure below cliff section showing soft-sediment deformation in grey Westbury Formation mudstones,
 1217 basal Cotham Member sandstone thickening away from Fault A, mounded and contorted wavy-bedded
 1218 sandstones immediately above the basal sandstone.

1219 **e**, Basal sandstone of Cotham Member showing contorted cross-bedded sand from its base mixed into
 1220 deformed mudstone of the underlying Westbury Formation.

1221 **f**, Minor fault offsetting the base of the Cotham Member, downthrow to right. Contorted wavy-bedded
 1222 sandstones overlying the basal sandstone to the right are absent on the downthrown side. The grey-brown
 1223 homogenous silty mudstone overlying the basal sandstone shows whisps and inclusions of black mudstone,
 1224 some of which appears to have flowed across the fault plane (centre of image). Note the stub of sandstone
 1225 (lower right) on the ‘wrong’ side of the fault. Ruler = 30 cm in **d–f**.

1226

1227 **Figure 7**. Cloghfin Port, Islandmagee. Sketch map of Penarth Group outcrop at Cloghfin Port, with
 1228 measured sections (1–11) through Westbury Formation (at top) to illustrate the influence of synsedimentary
 1229 fault movement on deposition and the stratigraphic constraints on the timing of fault movement.

1230

1231 **Figure 8**. Correlation of coastal exposures of the Triassic-Jurassic boundary succession in south-east
 1232 County Antrim. Sample levels indicated in the Cloghan Point (Whitehead), Cloghfin Port and The Gobbins
 1233 sections are those used in Steinhorsdottir et al. (2011), with their correlative positions indicated against the
 1234 continuous Waterloo Bay section.

1235 **Figure 9 a–d**. Cotham Member at Waterloo Bay.

1236 **a**, Basal sandstone of Cotham Member above dark mudstone of Westbury Formation. Note highly contorted
 1237 sand-mud alternations above basal sandstone, with large recumbent fold at top right.

1238 **b–d**, all from top 1.2 m of lower Cotham Member.

1239 **b**, Tidalite of mud-silt couplets with alternating planar-bedded and rippled units. Ripples across centre of
 1240 image have bidirectional mud drapes indicating flow-ebb current reversal.

1241 **c**, Top of lower Cotham Member, with ruler at upper limit of soft sediment deformation. Blue arrow
 1242 indicates sandstone bed overlying ‘mud-cracked’ horizon; white arrows indicate erosion surface on a channel
 1243 flank.

1244 **d**, Tidalite ~40 cm below ‘mud-cracked’ surface, with bundles of very finely interlaminated sand and mud
 1245 alternating with mud-dominated units. Ruler is 30 cm in all images.

1246

1247 **Figure 10**. Summary of Triassic–Jurassic boundary events in south-east County Antrim. See text for further
 1248 explanation. The $p\text{CO}_2$ proxy data are derived from *Brachyphyllum* cuticle in Steinhorsdottir et al. (2011);
 1249 carbon stable-isotopes, seismicity and relative sea-level are from this study. The correlated position of the

1250 Triassic–Jurassic boundary is indicated by the red horizontal line according to option 1 (see Figure 12 and
 1251 text).

1252

1253 **Figure 11 a–c.** Subaqueous sedimentary cracks at ‘mud-cracked’ surface in Cotham Member, Waterloo Bay.

1254 **a,** Top surface of ‘mud-cracked’ horizon.

1255 **b,** Vertical section, with ‘mud-cracked’ surface indicated by blue arrow. White arrow to left indicates a low-
 1256 angle crack which kinks to follow bedding and then kinks downward again. White arrow to right indicates
 1257 small ptigmatic intersecting cracks.

1258 **c,** Vertical section through ‘mud-cracked’ surface (blue arrow), with white arrow indicating large low-angle
 1259 anastomosing crack. Note continuity of sedimentation across surface and deformed cross-laminated sets
 1260 (lower right).

1261

1262 **Figure 12.** Correlation of the Waterloo Bay carbon stable-isotope curve with curves from the TJB GSSP
 1263 section at Kujoch, the Tiefengraben (Eiberg Basin) section and the St Audrie’s Bay and Doniford Bay
 1264 sections in the Bristol Channel Basin. The Tiefengraben and Kujoch isotope curves have been correlated by
 1265 palynology (see Hillebrandt et al., 2013). Tiefengraben simplified isotopes and biostratigraphical markers
 1266 after Kürschner et al. (2007), Kujoch simplified lithostratigraphy and isotopes after Hillebrandt et al. (2013).
 1267 Note that the start of the ‘main’ excursion is missing in the Kujoch curve due to a fault omitting strata near to
 1268 the top of the Schattwald Beds (indicated in pink) and the points joined by the blue line in the Tiefengraben
 1269 curve are from the Eiberg section. St Audrie’s Bay carbon stable-isotopes are after Hesselbo et al. (2002,
 1270 2004), biostratigraphic markers after Warrington et al. (2008). Doniford Bay carbon stable-isotopes,
 1271 lithostratigraphy (simplified) and biostratigraphic markers are after Clémence et al. (2010). The Doniford
 1272 Bay and St Audrie’s Bay isotope curves are to the same vertical scale, whilst the Waterloo Bay curve is
 1273 reduced by 50% relative to them. The Triassic–Jurassic boundary (TJB) marked by the first appearance of
 1274 *Psiloceras spelae tyrolicum* at Kujoch is indicated by the green line, with correlation Level 1, Level 2 and
 1275 Level 3 being shown. The negative shift of the ‘initial’ and ‘main’ CIE intervals are indicated with blue
 1276 shading. Letters A–C indicate features of the isotope curves discussed in the main text. *Psiloceras erugatum*
 1277 is correlated with *P. calliphyllum* after Hillebrandt and Kment (2015).

Figure 1

[Click here to access/download;Figure;Jeram et al Fig 1.jpg](#)

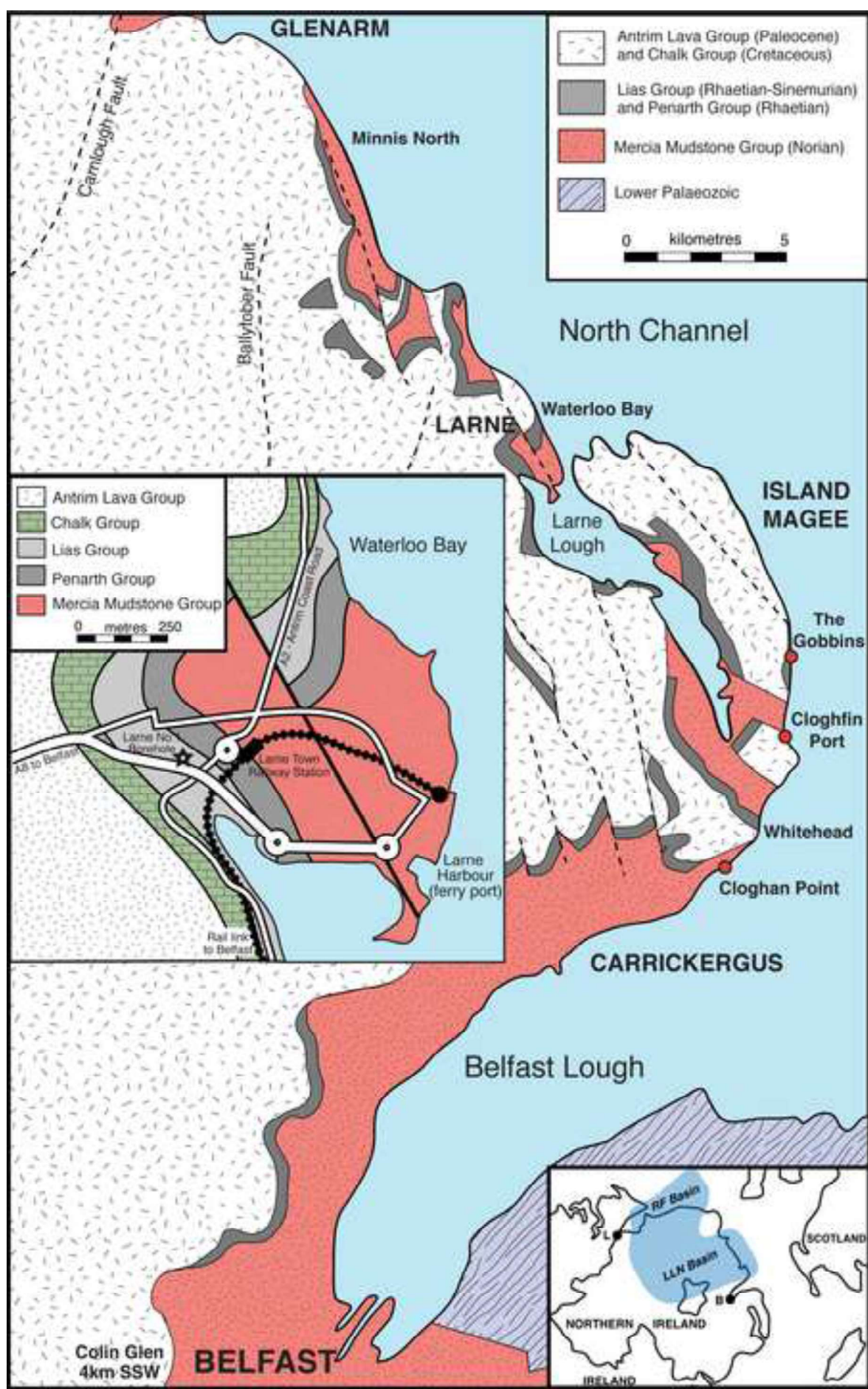
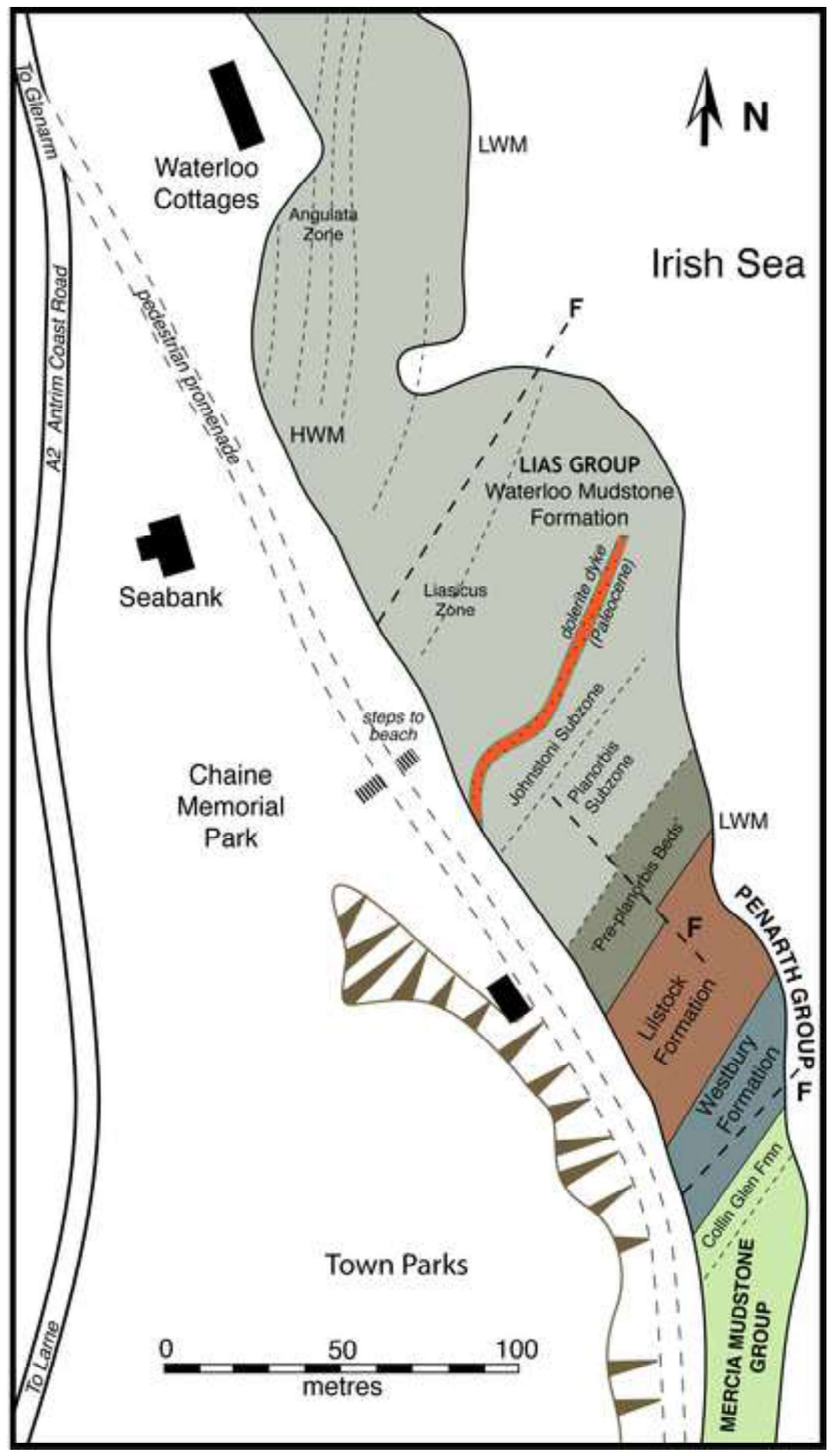
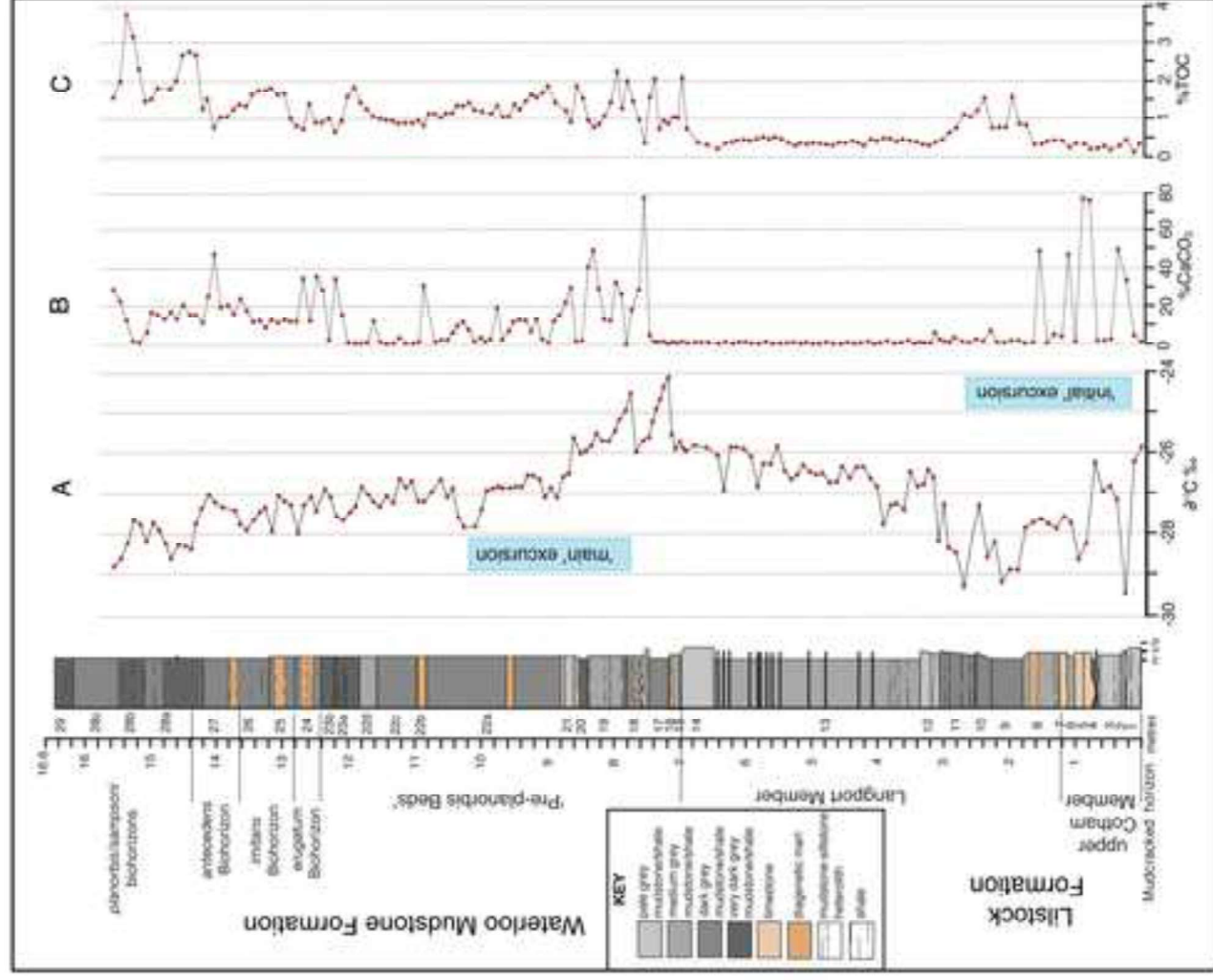
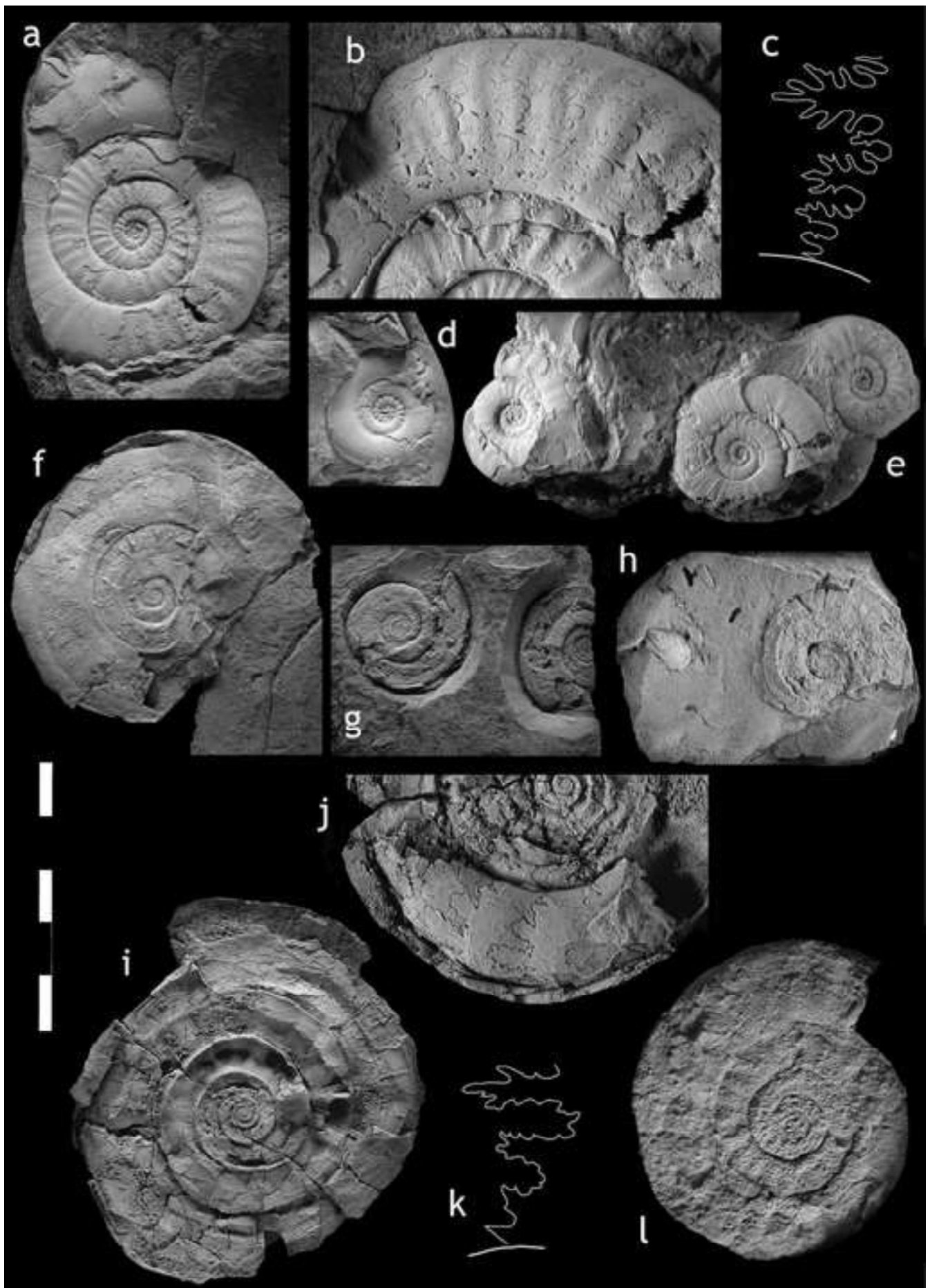


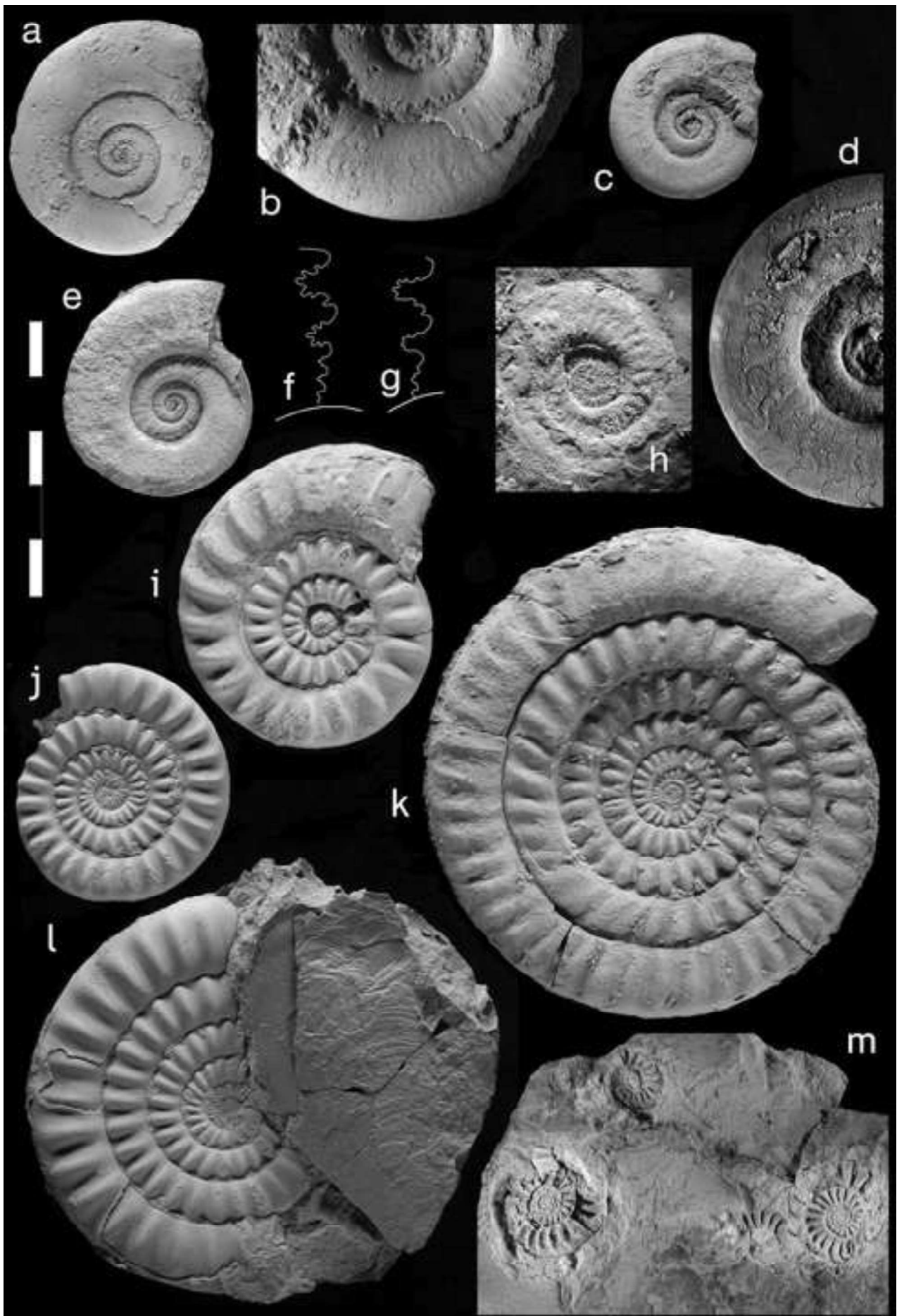
Figure 2

[Click here to access/download;Figure;Jeram et al Fig 2.jpg](#)









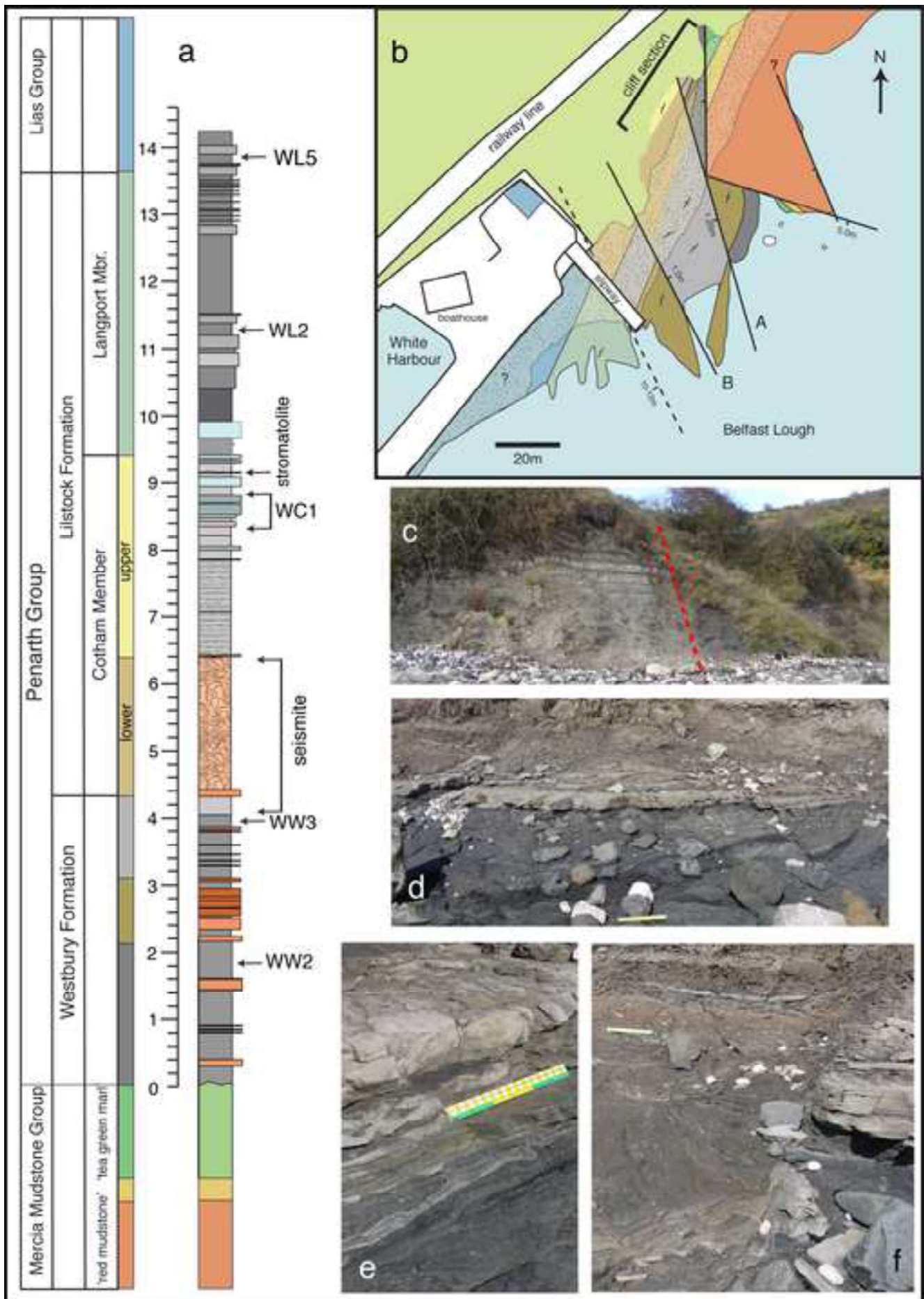
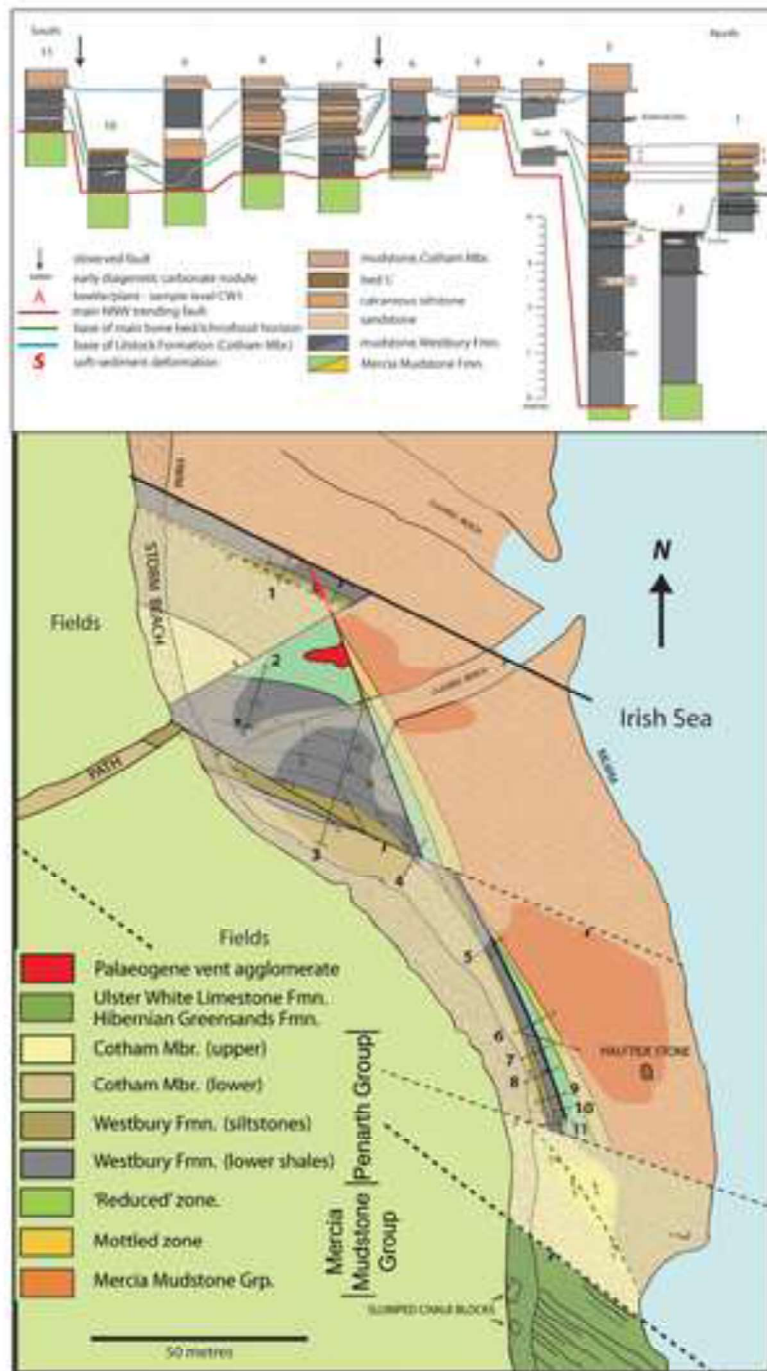
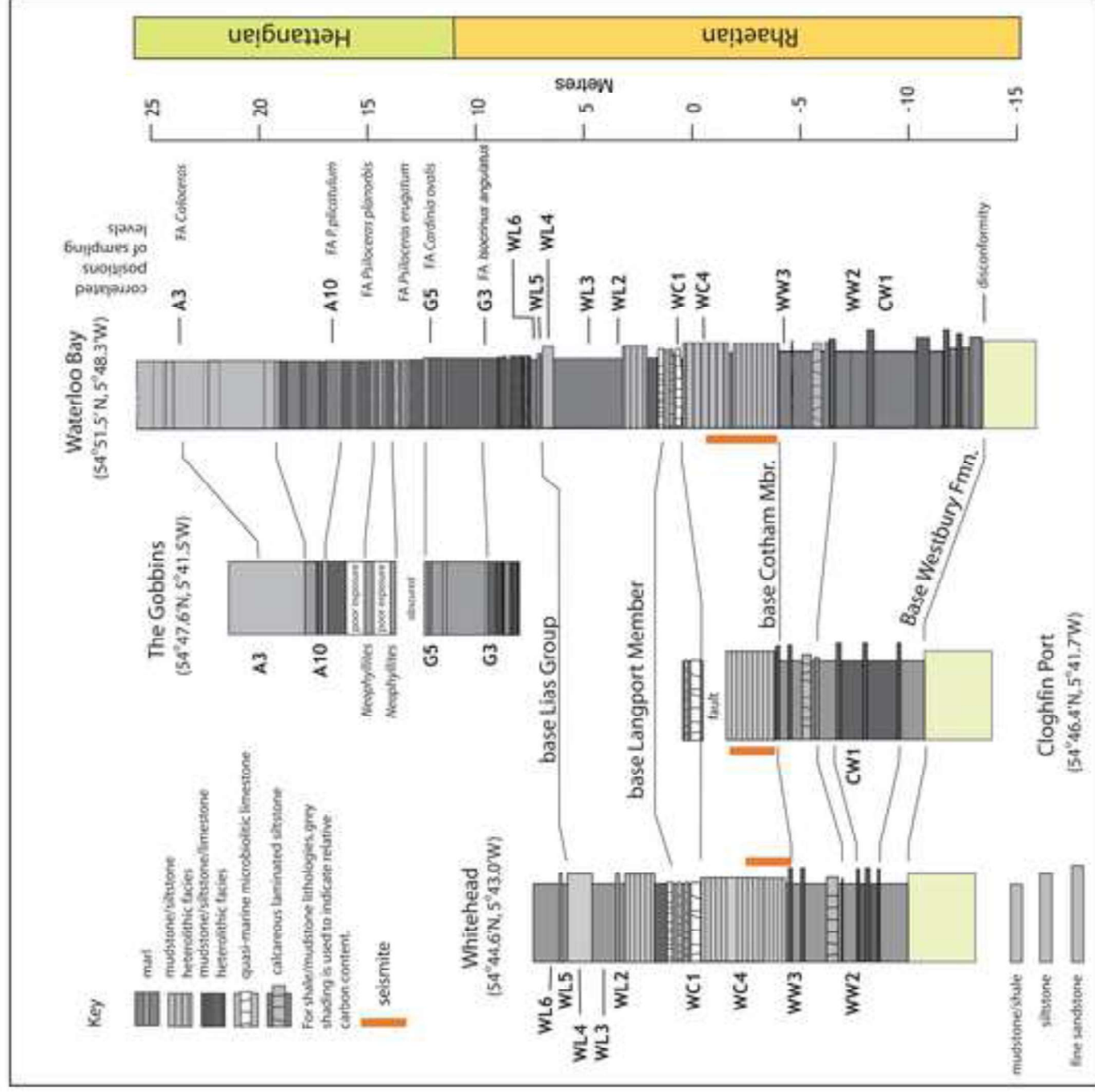


Figure 7

[Click here to access/download;Figure;Jeram et al Fig 7.jpg](#)





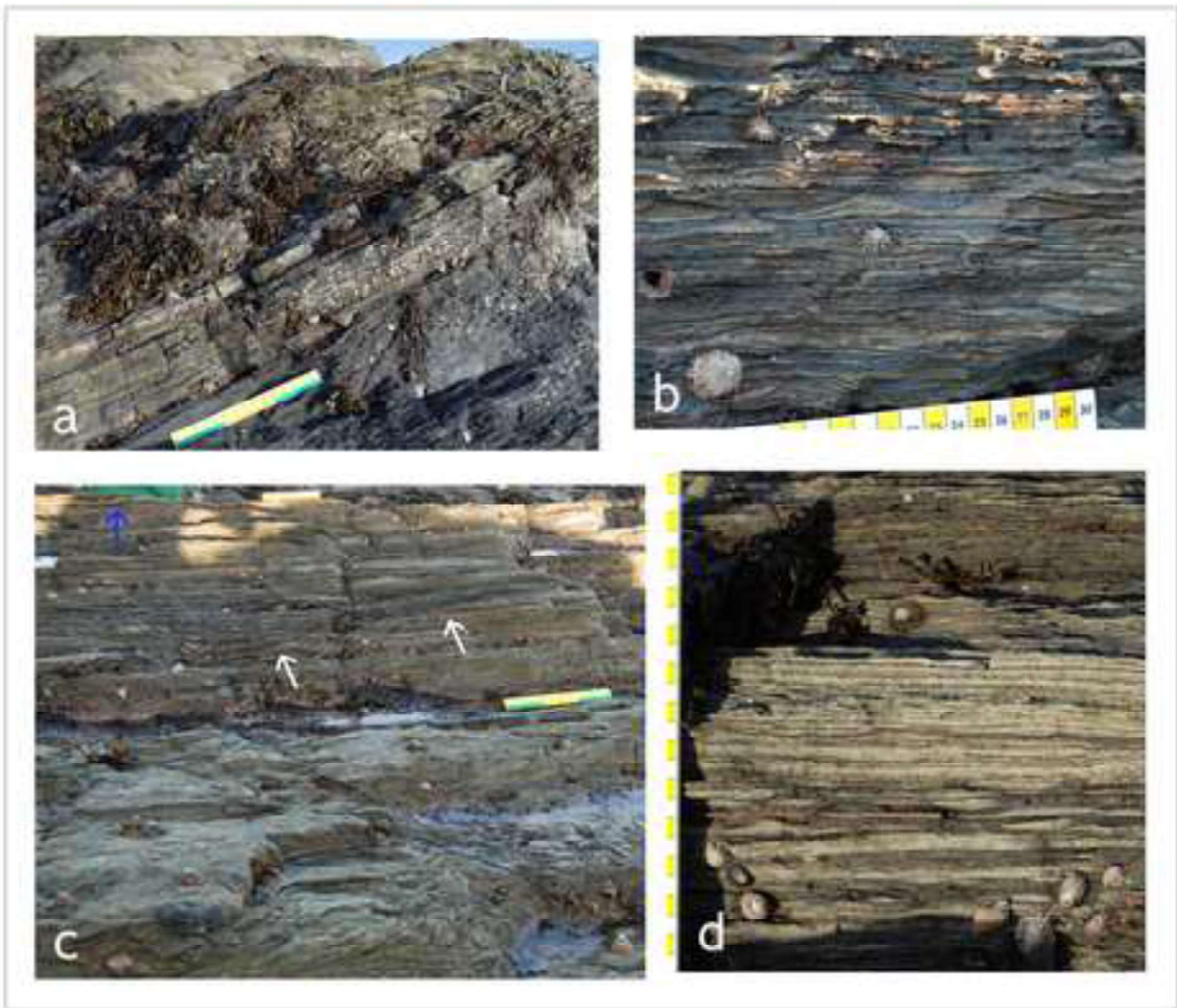
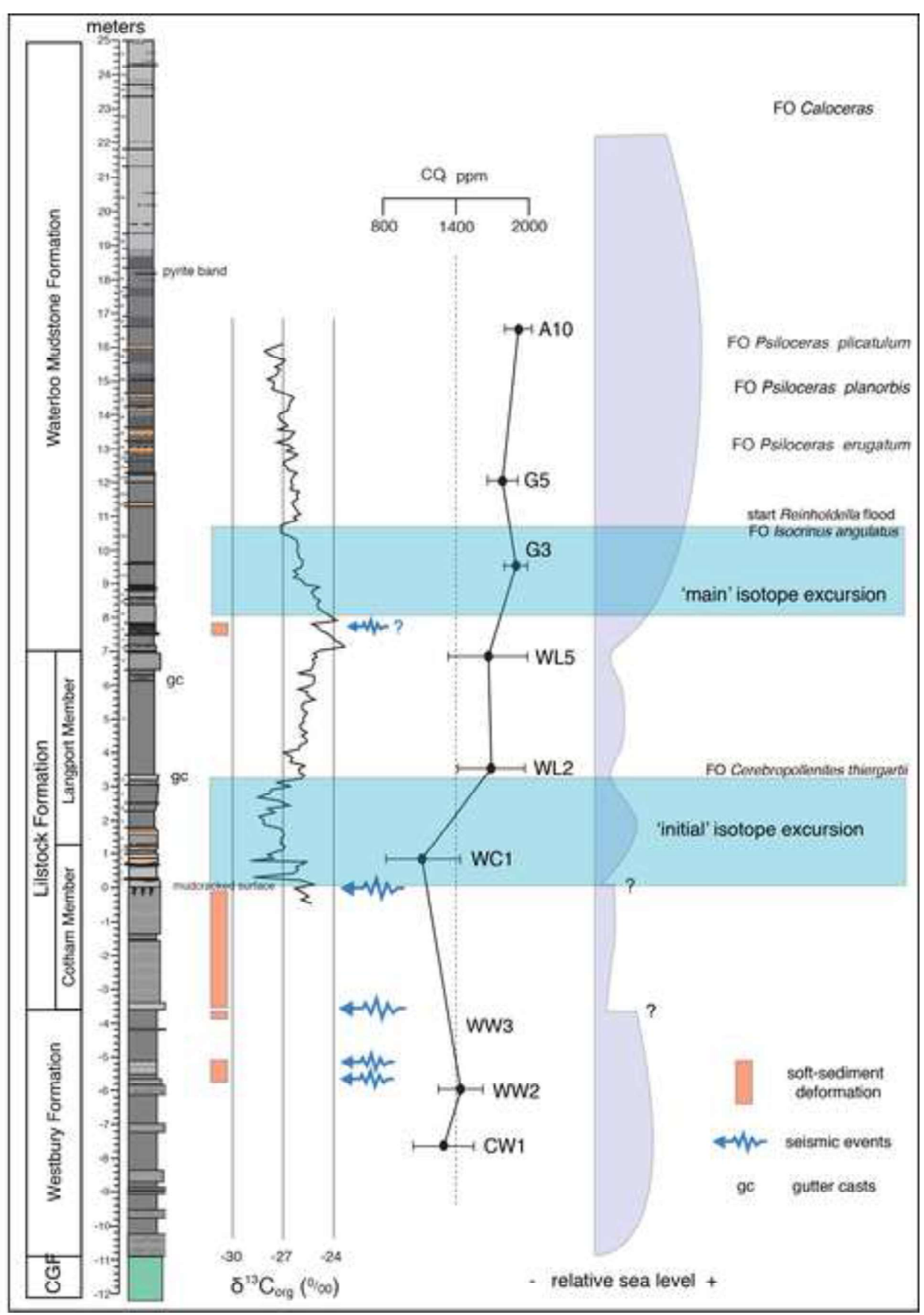
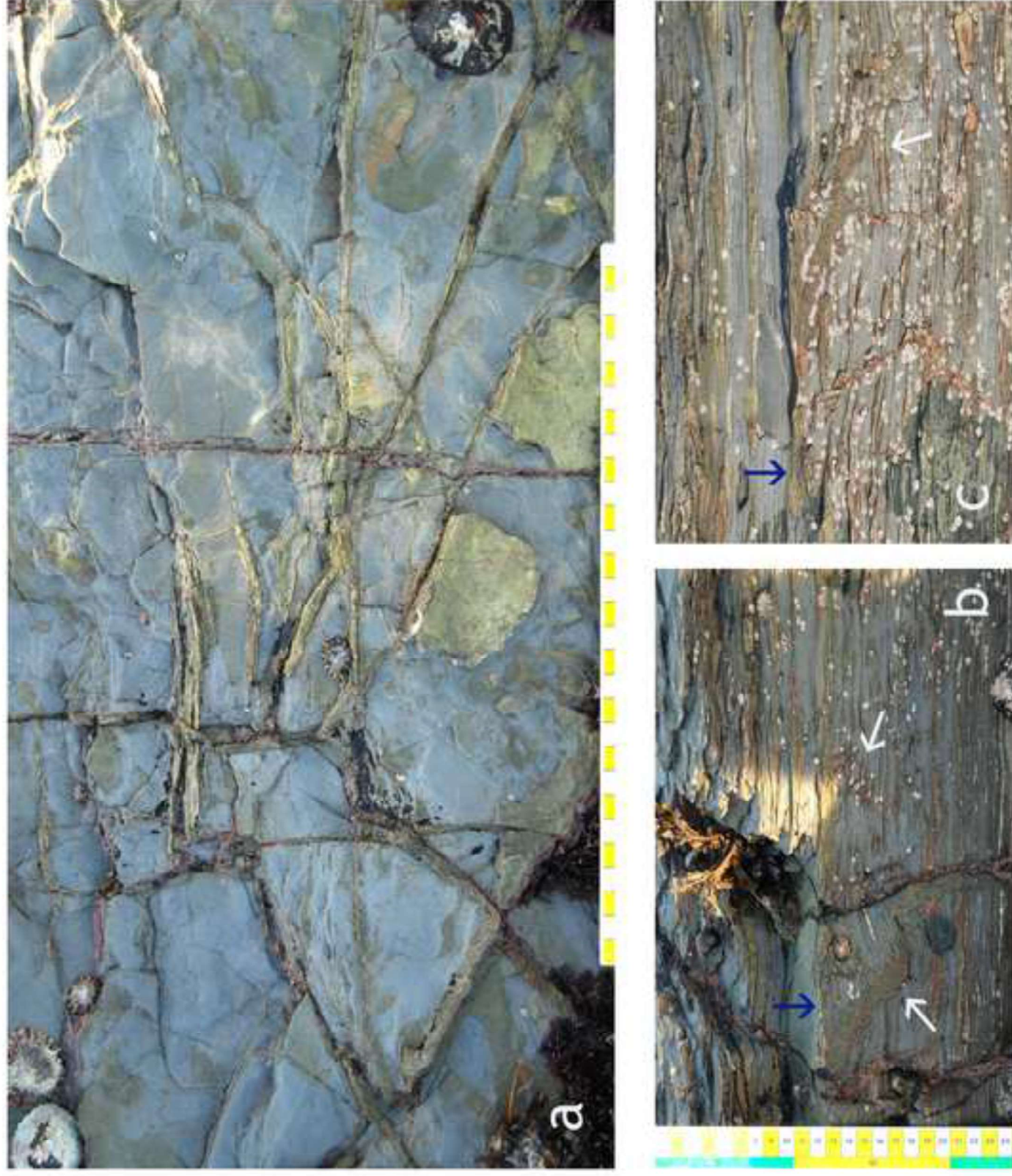


Figure 10

[Click here to access/download;Figure;Jeram et al Fig 10.jpg](#)





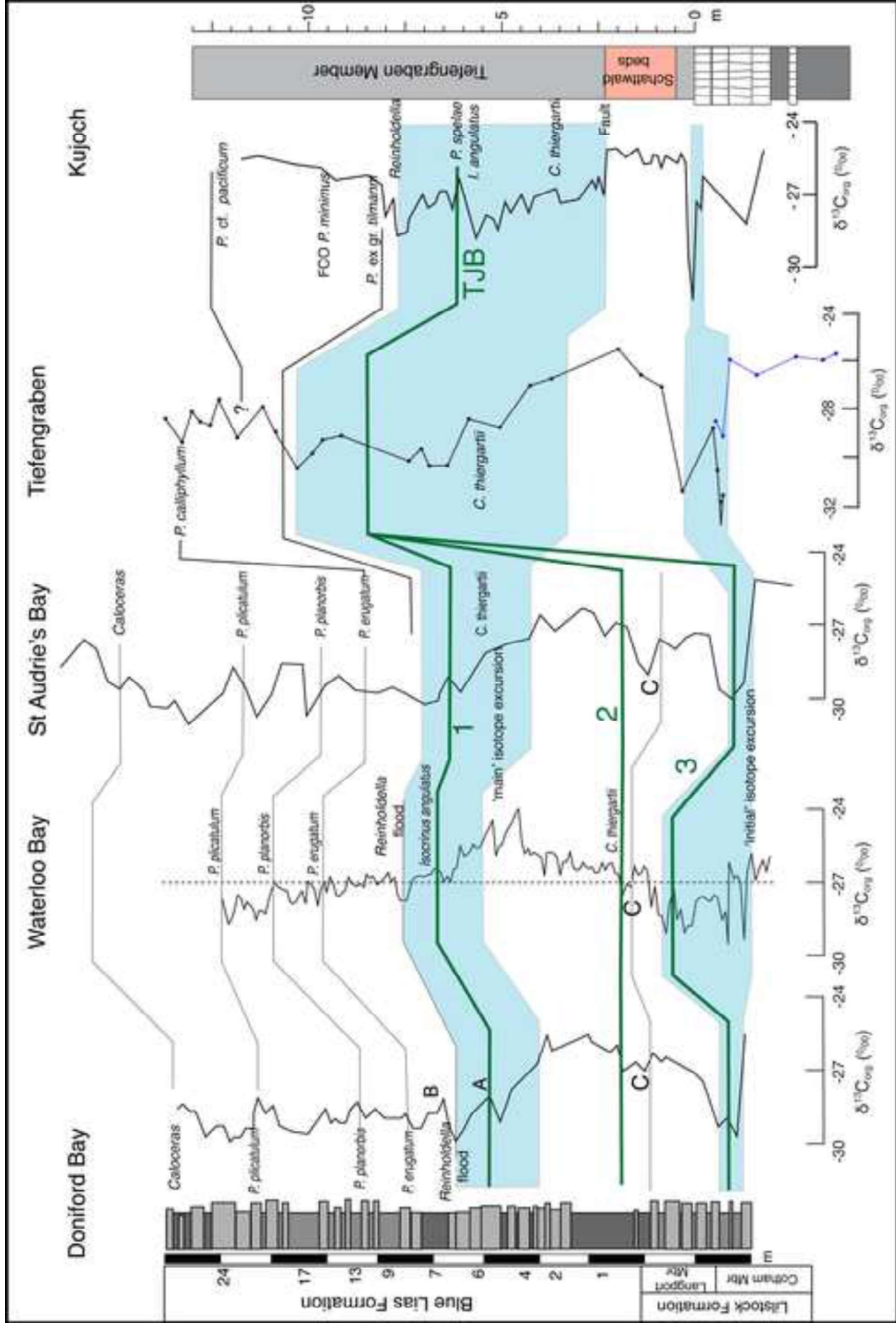


Figure 12